A novel computational pipeline for *var* gene expression augments the discovery of changes in the *Plasmodium falciparum* transcriptome during transition from *in vivo* to short-term *in vitro* culture

Clare Andradi-Brown[1,2,3], Jan Stephan Wichers-Misterek[4-6], Heidrun von Thien[4-6], Yannick D. Höppner[4-6], Judith A. M. Scholz[4], Helle Smedegaard Hansson[7], Emma Filtenborg Hocke[7], Tim-Wolf Gilberger[4-6], Michael F. Duffy[8], Thomas Lavstsen[7], Jake Baum[2,9], Thomas D. Otto[10*], Aubrey J. Cunnington[1,3*¥], Anna Bachmann[4-6,11*¥]

[1] Section of Paediatric Infectious Disease, Department of Infectious Disease, Imperial College London, UK
[2]Department of Life Sciences, Imperial College London, South Kensington, London, SW7 2AZ, UK
[3]Centre for Paediatrics and Child Health, Imperial College London, UK
[4]Bernhard Nocht Institute for Tropical Medicine, Bernhard-Nocht-Strasse 74, 20359 Hamburg, Germany;
[5]Centre for Structural Systems Biology, Hamburg, Germany, Notkestraße 85, 22607 Hamburg, Germany;
[6]Biology Department, University of Hamburg, Hamburg, Germany;
[7]CMP, University of Copenhagen, 2200 Copenhagen, Denmark;
[8]Department of Microbiology and Immunology, University of Melbourne, Melbourne/Parkville VIC 3052, Australia;
[9]School of Biomedical Sciences, Faculty of Medicine & Health, UNSW, Kensington, Sydney, 2052, Australia
[10]School of Infection & Immunity, MVLS, University of Glasgow, UK
[11]German Center for Infection Research (DZIF), partner site Hamburg-Borstel-Lübeck-Riems, Germany
*Equal contribution
[¥]To whom correspondence should be addressed

Corresponding authors:
Aubrey Cunnington, Section of Paediatric Infectious Disease, Department of Infectious Disease, Imperial College London, Norfolk Place, W2 1PG, London, UK. a.cunnington@imperial.ac.uk
Anna Bachmann, Bernhard Nocht Institute for Tropical Medicine, Bernhard-Nocht-Strasse 74, 20359 Hamburg, Germany. bachmann@bni-hamburg.de

Abstract

The pathogenesis of severe *Plasmodium falciparum* malaria involves cytoadhesive microvascular sequestration of infected erythrocytes, mediated by *P. falciparum* erythrocyte membrane protein 1 (PfEMP1). PfEMP1 variants are encoded by the highly polymorphic family of *var* genes, the sequences of which are largely unknown in clinical samples. Previously, we published new approaches for *var* gene profiling and classification of predicted binding phenotypes in clinical *P. falciparum* isolates (Wichers *et al.*, 2021), which represented a major technical advance. Building on this, we report here a novel method for *var* gene assembly and multidimensional quantification from RNA-sequencing that even outperforms the earlier approach of Wichers et al., 2021 on both laboratory and clinical isolates across a combination of metrics. It is a powerful tool to interrogate the *var* transcriptome in context with the rest of the transcriptome and can be applied to enhance our understanding of the role of *var* genes in malaria pathogenesis. We applied this new method to investigate changes in *var* gene expression through early transition to *in vitro* culture, using paired sets of *ex vivo* samples from our previous study, cultured for up to three generations. In parallel, changes in non-polymorphic core gene expression were investigated. Unpredictable *var* gene switching and convergence towards *var2csa* were observed in culture, along with differential expression of 19% of the core transcriptome between paired *ex vivo* and generation 1 samples. Our results cast doubt on the validity of the common practice of using short-term cultured parasites to make inferences about *in vivo* phenotype and behaviour.

Introduction

Malaria is a parasitic life-threatening disease caused by species of the *Plasmodium* genus. In 2021, there were an estimated 619,000 deaths due to malaria, with children under 5 accounting for 77% of these (WHO, 2022). *Plasmodium falciparum* causes the greatest disease burden and most severe outcomes. *P. falciparum* has several highly polymorphic variant surface antigens (VSA) encoded by multi-gene families, with the best studied high molecular weight *Plasmodium falciparum* erythrocyte membrane protein 1 (PfEMP1) family of proteins known to play a major role in the pathogenesis of malaria (Leech *et al.*, 1984, Wahlgren *et al.*, 2017). About 60 *var* genes per parasite genome encode different PfEMP1 variants, which are exported to the surface of parasite-infected erythrocytes, where they mediate cytoadherence to host endothelial cells (Leech *et al.*, 1984, Su *et al.*, 1995, Smith *et al.*, 1995, Baruch *et al.*, 1995, Rask *et al.*, 2010). *Var* genes are expressed in a mutually exclusive pattern, resulting in each parasite expressing only one *var* gene, and therefore one PfEMP1 protein, at a time (Scherf *et al.*, 1998). Due to the exposure of PfEMP1 proteins to the host immune system, switching expression between the approximately 60 *var* genes in the genome is an effective immune evasion strategy, which can result in selection and dominance of parasites expressing particular *var* genes within each host (Smith *et al.*, 1995).

The polymorphic *var* genes were classified into four categories (A, B, C, and E) according to their chromosomal location, transcriptional direction, type of 5'-upstream sequence (UPSA–E) (Figure 1a and b) (Lavstsen *et al.*, 2003, Kraemer & Smith, 2003, Kyes *et al.*, 2007, Rask *et al.*, 2010). PfEMP1 proteins have up to 10 extracellular domains, with the N-terminal domains forming a semi-conserved head structure complex typically containing the N-terminal segment (NTS), a Duffy binding-like domain of class α (DBLα) coupled to a cysteine-rich interdomain region (CIDR). C-terminally to this head structure, PfEMP1 exhibit a varying but semi-ordered composition of additional DBL and CIDR domains of different subtypes (Figure 1c). The PfEMP1 family divide into three main groups based on the receptor specificity of the N-terminal CIDR domain. PfEMP1 with CIDRα1 domains bind EPCR, while PfEMP1 with CIDRα2-6 domains bind CD36 and the atypical VAR2CSA PfEMP1 bind placental CSA (Salanti *et al.*, 2004). In addition to these, a subset of PfEMP1 have N-terminal CIDRβ/γ/δ domains of unknown function. This functional diversification correlates with the genetic organization of the *var* genes. Thus, UPSA *var* genes encode PfEMP1 with domain sub-variants NTSA-DBLα1-CIDRα1/β/γ/δ, whereas UPSB and UPSC *var* genes encode PfEMP1 with NTSB-DBLα0-CIDRα2-6. One exception to this rule is the B/A chimeric *var* genes, which encode NTSB-DBLα2-CIDRα1 domains. The different receptor binding specificities are associated with different clinical outcome of infection. Pregnancy-associated malaria is linked to parasites expressing VAR2CSA, whereas parasites expressing EPCR-binding PfEMP1 are linked to severe malaria and parasites expressing CD36 binding PfEMP1 are linked to uncomplicated malaria (Turner *et al.*, 2013, Lavstsen *et al.*, 2012, Avril *et al.*, 2012, Claessens *et al.*, 2012, Tonkin-Hill *et al.*, 2018, Wichers *et al.*, 2021). The clinical relevance of PfEMP1 with unknown head structure functions and the PfEMP1 C-terminal domains is largely unknown, albeit both specific endothelial receptor and plasma protein interactions have been described (Tuikue Ndam *et al.*, 2017, Quintana *et al.*, 2019, Stevenson *et al.*, 2015). Each parasite genome carries a similar repertoire of *var* genes, which in addition to the described variants include the highly conserved *var1* pseudogene, which in most genomes occur with no or a truncated exon 2. Also, most genomes carry the unusually small and highly conserved *var3* genes, of unknown function.

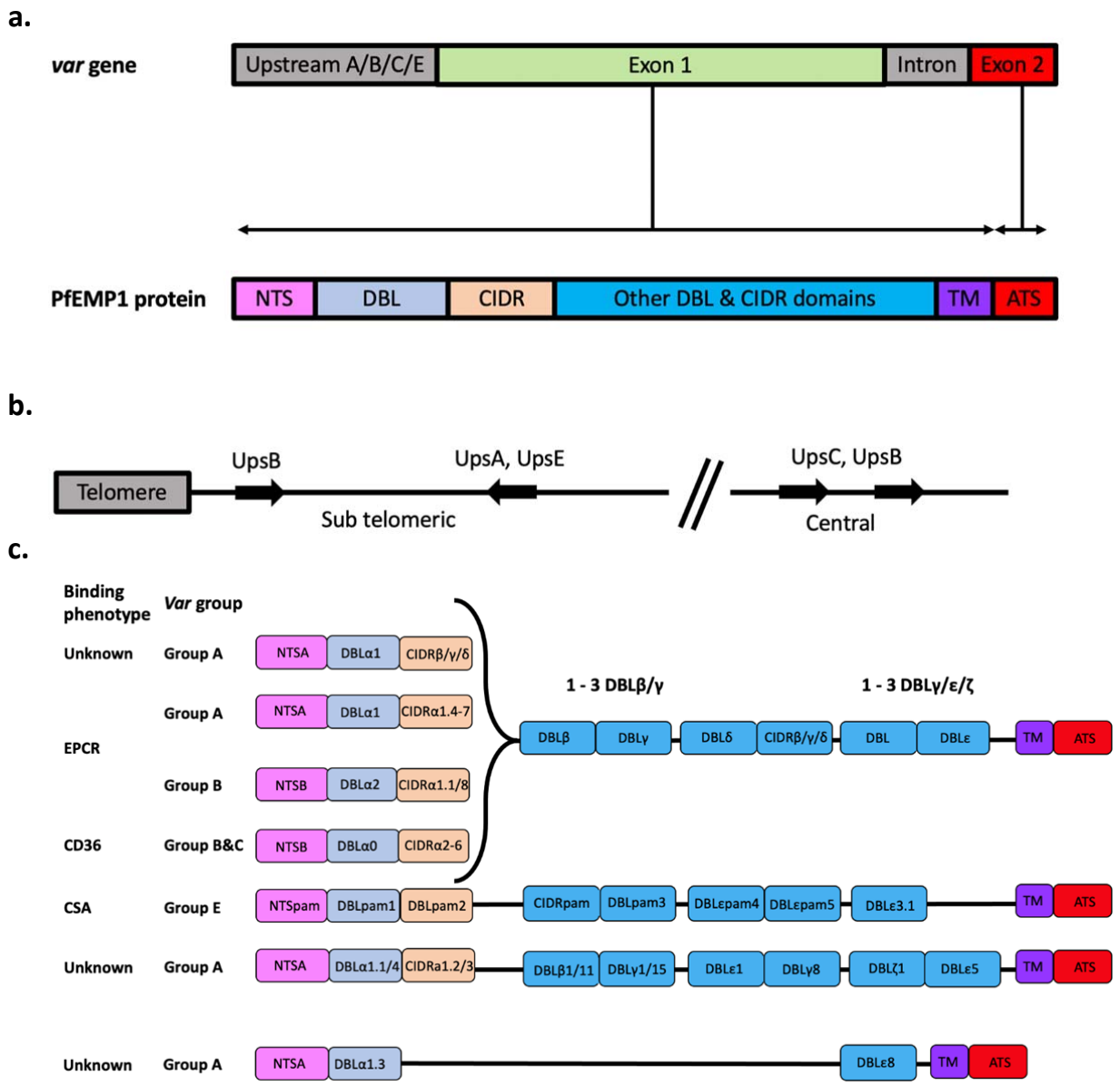

Figure 1: Summary of the *var* gene, PfEMP1 protein structure, *var* chromosomal location and PfEMP1 binding phenotypes. a) Structure of the *var* gene which encodes the PfEMP1 protein. The *var* gene is composed of two exons, the first, around 3–9.4 kb, encodes the highly variable extracellular region and the transmembrane region (TM) of PfEMP1. Exon 2 is shorter with about 1.2 kb and encodes a semi-conserved intracellular region (acidic terminal segment, ATS). The PfEMP1 protein is composed of an N-terminal segment (NTS), followed by a variable number of Duffy binding-like (DBL) domains and a cysteine-rich interdomain region (CIDR) (Rask et al., 2010). **b)** Chromosomal position and transcriptional direction (indicated by arrows) of the different *var* gene groups, designated by the respective type of upstream sequence (Deitsch & Hviid, 2004). **c)** Summary of PfEMP1 proteins encoded in the parasite genome, their composition of domain subtypes and associated N-terminal binding phenotype. Group A and some B proteins have an EPCR-binding phenotype; the vast majority of group B and C PfEMP1 proteins bind to CD36. Group A proteins also include those that bind an as yet unknown receptor, as well as VAR1 and VAR3 variants with unknown function and binding phenotype. VAR2CSA (group E) binds placental CSA. Figure modified from Wichers et al., 2021.

Comprehensive characterisation and quantification of *var* gene expression in field samples have been complicated by biological and technical challenges. The extreme polymorphism of *var* genes precludes a reference *var* sequence, some *var* genes are lowly expressed or not expressed at all, contain repetitive domains and can have large duplications (Otto *et al.*, 2019). Consequently, most studies relating *var* gene expression to severe malaria have relied on primers with restricted coverage of the *var* family, use of laboratory-adapted parasite strains or have predicted the downstream sequence from DBLα domains (Sahu *et al.*, 2021, Storm *et al.*, 2019, Shabani *et al.*, 2017, Mkumbaye *et al.*, 2017, Kessler *et al.*, 2017, Bernabeu *et al.*, 2016, Jespersen *et al.*, 2016, Lavstsen *et al.*, 2012). This has resulted in incomplete *var*

gene expression quantification and the inability to elucidate specific or detect atypical *var* sequences. RNA-sequencing has the potential to overcome these limitations and secure a better link between *var* expression and PfEMP1 phenotpye in *in vitro* assays, co-expression with other polymorphic gene families, core genes and epigenetics, which the qPCR and DBLα-tag approaches are not suited for. More recent approaches for *var* assembly and quantification, based on RNA-sequencing, represent huge advancements compared to qPCR and DBLα-tag analyses. However, they still produce inadequate assembly of the biologically important N-terminal domain region, have a relatively high number of misassemblies and do not provide an adequate solution for handling the conserved *var* variants (Tonkin-Hill *et al.*, 2018, Wichers *et al.*, 2021, Guillochon *et al.*, 2022).

Plasmodium parasites from human blood samples are often adapted to or expanded through *in vitro* culture to provide sufficient parasites for subsequent investigation of parasite biology and phenotype (Brown & Guler, 2020). This is also the case for several studies assessing PfEMP1 phenotype of parasites isolated from malaria-infected donors (Pickford *et al.*, 2021, Joste *et al.*, 2020, Storm *et al.*, 2019, Tuikue Ndam *et al.*, 2017, Bruske *et al.*, 2016, Claessens *et al.*, 2012, Lavstsen *et al.*, 2005, Jensen *et al.*, 2004, Kirchgatter & Portillo Hdel, 2002, Dimonte *et al.*, 2016, Hoo *et al.*, 2019). However, *in vitro* conditions are considerably different to those found *in vivo,* having, for example different nutrient availability and lack of a host immune response (Brown & Guler, 2020). Previous studies found inconsistent results in terms of whether *var* gene expression was impacted by culture and if it was, they disagreed on which *var* groups were the most affected (Zhang *et al.*, 2011, Peters *et al.*, 2007). Similar challenges apply to the understanding of changes in *P. falciparum* non-polymorphic core genes in culture, with the focus previously being on long-term laboratory adapted parasites (Claessens *et al.*, 2017, Mackinnon *et al.*, 2009). Consequently, direct interpretation of a short-term cultured parasite's transcriptome remains a challenge. It is fundamental to understand *var* genes in context with the parasite's core transcriptome. This could provide insights into *var* gene regulation and phenomena such as the proposed lower level of *var* gene expression in asymptomatic individuals (Almelli *et al.*, 2014, Andrade *et al.*, 2020).

Here we present an improved method using RNA-sequencing data for assembly, characterization, and quantification of *var* gene expression. This new approach overcomes previous limitations and outperforms current methods, enabling a much greater understanding of the *var* transcriptome. We demonstrate the power of this new approach by evaluating changes in *var* gene expression of paired samples from clinical isolates *of P. falciparum* during their early transition to *in vitro* culture*,* across several generations. We also assess changes in relation to disease phenotype and prior malaria exposure status. The use of paired samples, which are genetically identical and hence have the same *var* gene repertoire, allows validation of assembled transcripts and direct comparisons of expression. We complement this with a comparison of changes which occur in the non-polymorphic core transcriptome over the same transition into culture. We find a background of modest changes in *var* gene expression with unpredictable patterns of *var* gene switching, favouring an apparent convergence towards *var2csa* expression. More extensive changes were observed in the core transcriptome during the first cycle of culture, suggestive of a parasite stress response.

143 **Results**

144 To extend our ability to characterise *var* gene expression profiles and changes over time in clinical *P.*
145 *falciparum* isolates, we set out to improve current assembly methods. Previous methods for assembling
146 *var* transcripts have focussed on assembling whole transcripts (Tonkin-Hill *et al.*, 2018, Wichers *et al.*,
147 2021, Guillochon *et al.*, 2022, Andrade *et al.*, 2020). However, due to the diversity within PfEMP1 domains,
148 their associations with disease severity and the fact they are not inherited together, a method that
149 focusses on domain assembly first was also developed. In addition, a novel whole transcript approach,
150 using a different *de novo* assembler, was developed and their performance compared to the method of
151 Wichers et al. (hereafter termed "the original approach", Figure 2). The new approaches made use of the
152 MalariaGEN *P. falciparum* dataset, which led to the identification of additional multi-mapping non-core
153 reads (a median of 3,955 reads per sample) prior to *var* transcript assembly (MalariaGen *et al.*, 2021). We
154 incorporated read error correction and improved large scaffold construction with fewer misassemblies (see
155 Methods). We then applied this pipeline to paired *ex vivo* and short-term *in vitro* cultured parasites to
156 enhance our understanding of the impact of short-term culturing on the *var* transcriptome (Figure 3). The
157 *var* transcriptome was assessed at several complementary levels. First, *var* transcript and domain
158 differential expression was performed. Next, changes in the dominantly expressed *var* gene and the
159 homogeneity of *var* expression in paired samples were investigated. Finally, *var* group and global *var* gene
160 expression changes were evaluated. This was accompanied by analysis of the core transcriptome through
161 short-term culture.

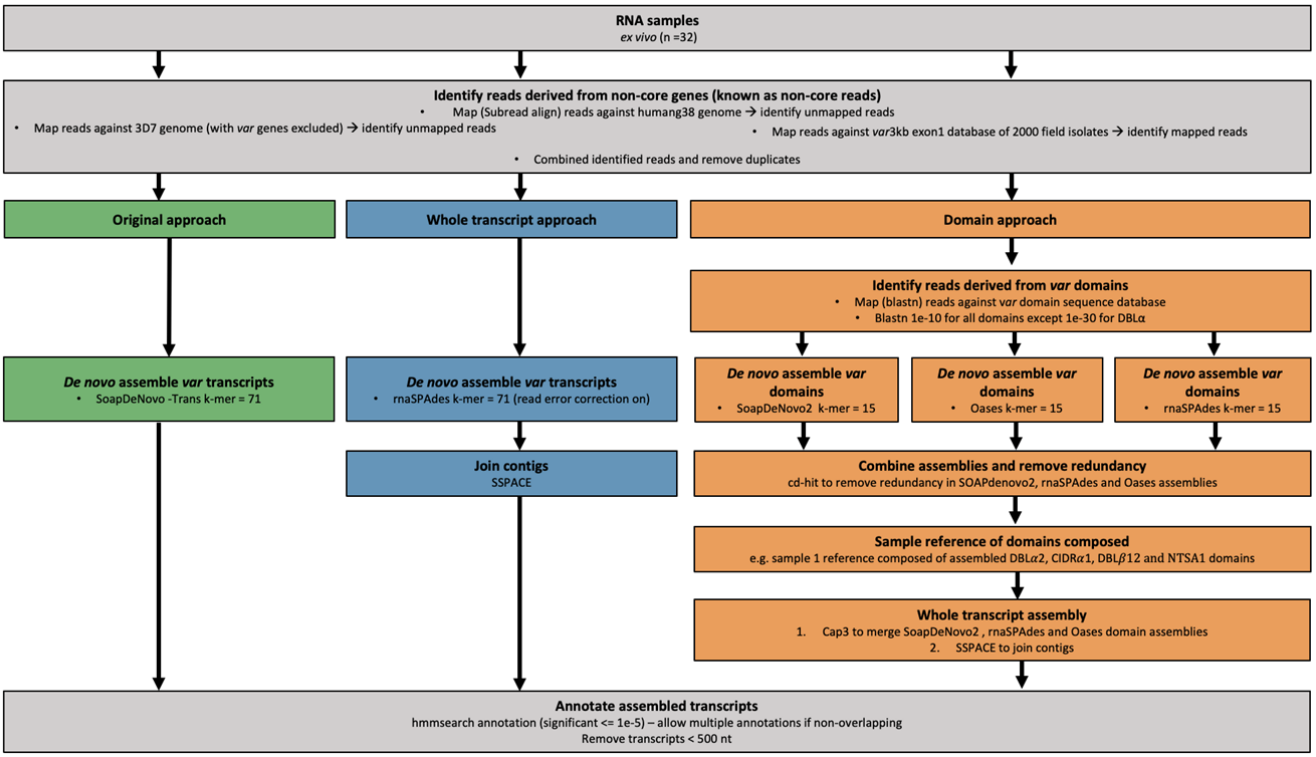

Figure 2: Novel computational pipelines for assembling *var* transcripts. The original approach (green) used SoapDeNovo-Trans (k=71) to perform whole *var* transcript assembly. The whole transcript approach (blue) focused on assembling whole *var* transcripts from the non-core reads using rnaSPAdes (k = 71). Contigs were then joined into longer transcripts using SSPACE. The domain approach (orange) assembled *var* domains first and then joined the domains into whole transcripts. Domains were assembled separately using three different *de novo* assemblers (SoapDeNovo2, Oases and rnaSPAdes). Next, a reference of assembled domains was composed and cd-hit (at sequence identity = 99%) was used to remove redundant sequences. Cap3 was used to merge and extend domain assemblies. Finally, SSPACE was used to join domains together. HMM models built on the Rask et al., 2010 dataset were used to annotate the assembled transcripts (Rask *et al.*, 2010). The most significant alignment was taken as the best annotation for each region of the assembled transcript (significance <= 1e-5) (identified using cath-resolve-hits0. Transcripts < 500nt were removed. A *var* transcript was selected if it contained at least one significantly annotated domain (in exon 1). *Var* transcripts that encoded only the more conserved exon 2 (ATS domain) were discarded. The three pipelines were run on the 32 malaria patient *ex vivo* samples from Wichers et al., 2021 (Wichers *et al.*, 2021).

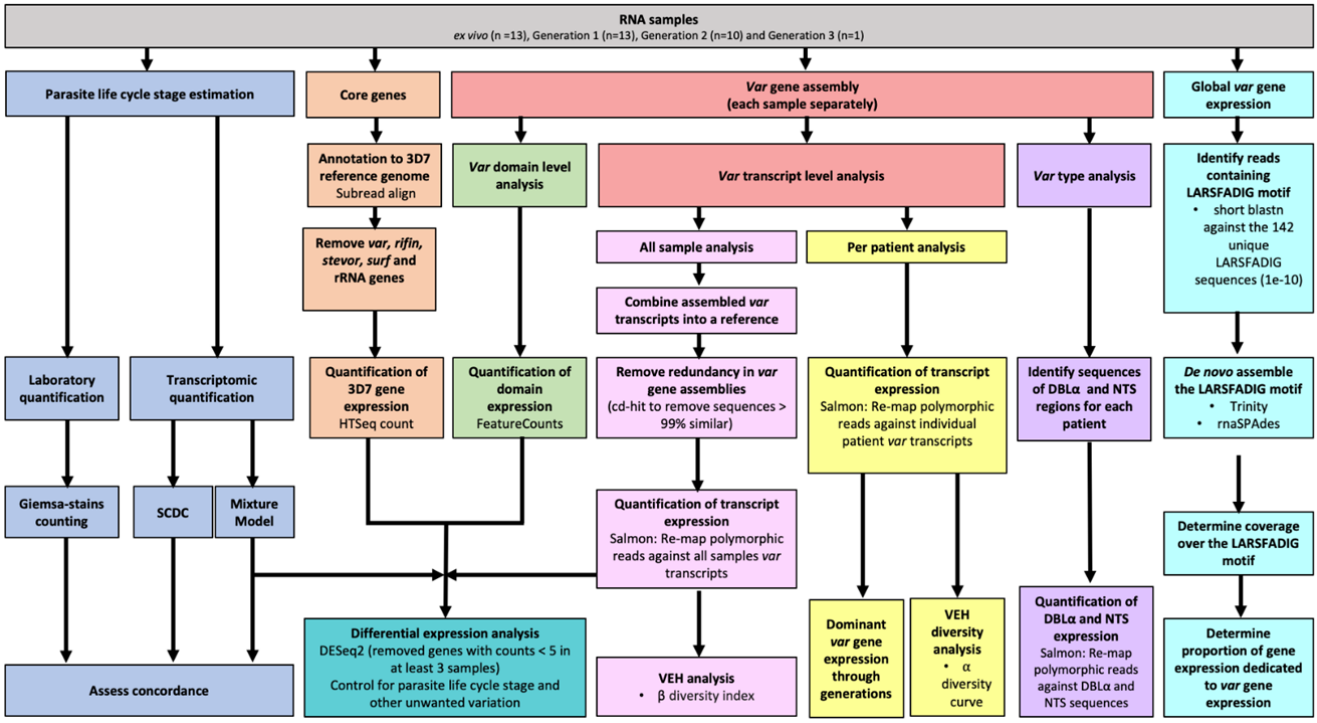

Figure 3: Summary of analyses of *var* and core gene transcriptome changes in paired *ex vivo* and short-term *in vitro* cultured parasites. From a total of 13 parasite isolates, the *ex vivo* samples (Wichers et al., 2021) and the corresponding *in vitro*-cultured parasites of the first (n=13), second (n=10) and third (n=1) replication cycle were analysed by RNA sequencing. The expression of non-polymorphic core genes and polymorphic *var* genes was determined in different analysis streams: (1) Non-polymorphic core gene reads were mapped to the 3D7 reference genome, expression was quantified using HTSeq and differential expression analysis performed (orange); (2) Polymorphic reads were identified, whole transcripts were assembled with rnaSPAdes, expression of both *var* transcripts (red) and domains (green) was quantified, and differential expression analysis was performed. All assembled *var* transcripts from all samples are combined in the 'all sample analysis' (pink) and this reference is used to quantify *var* transcript expression (previously described in Wichers et al., 2021). 'Per patient analysis' (yellow) represents combining all assembled *var* transcripts for samples originating from the same *ex vivo* sample only. *Var* type (Group A vs Group B and C) expression (purple) was quantified using the DBLα and NTS assembled sequences and differences across generations were assessed. Total *var* gene expression (turquoise) was quantified by assembling and quantifying the coverage over the highly conserved LARSFADIG motif, with the performance of assembly using Trinity and rnaSPAdes assessed. *Var* expression homogeneity (VEH) was analysed at the patient level (α diversity curves) and across all samples (β diversity index). All differential expression analyses were performed using DESeq2.To ensure a fair comparison of samples, which may contain different proportions of life cycle stages, the performance of two different *in silico* approaches was evaluated by counting Giemsa-stained thin blood smears (blue).

Improving *var* transcript assembly, annotation and quantification

A laboratory and a clinical dataset were used to assess the performance of the different *var* assembly pipelines (Figure 2). The laboratory dataset was a *P. falciparum* 3D7 time course RNA-sequencing dataset (ENA: PRJEB31535) (Wichers *et al.*, 2019). The clinical dataset contained samples from 32 adult malaria patients, hospitalised in Hamburg, Germany. 15 were malaria naïve and 17 were previously exposed to malaria. Eight of the malaria naïve patients went on to develop severe malaria and 24 had non-severe malaria (Wichers *et al.*, 2021).

Our i) new whole transcript approach, ii) domain assembly approach, and iii) modified version of the original approach were first applied to the *P. falciparum* 3D7 time course RNA-sequencing dataset to benchmark their performance (European nucleotide archive (ENA): PRJEB31535) (Wichers *et al.*, 2019) (Figure S1). The whole transcript approach performed best, achieving near perfect alignment scores for the dominantly expressed *var* gene. The domain and the original approach produced shorter contigs and required more contigs to assemble the *var* transcripts at the 8 and 16 hour post-invasion time points, when *var* gene expression is maximal (Figure S1c, f, g and h). However, we found high accuracies (> 0.95) across all approaches, meaning the sequences we assembled were correct (Figure S1b). The whole transcript approach also performed the best when assembling the lower expressed *var* genes (Figure S1e) and

180 produced the fewest misassemblies compared to the original approach (14 vs 19 respectively), especially
181 for the ring-stage samples (Table S1).
182
183 Next, the assembled transcripts produced from the original approach of Wichers *et al.*, 2021 were
184 compared to those produced from our new whole transcript and domain assembly approaches for *ex vivo*
185 samples from German travellers. Summary statistics are shown in Table 1. The whole transcript approach
186 produced the fewest transcripts, but of greater length than the domain approach and the original
187 approach (Figure S2). The whole transcript approach also returned the largest N50 score, which means that
188 it was the most contiguous assembly produced. The original approach and the new whole transcript
189 approach gave similar results for domain expression in each sample with greater correlation in results
190 observed between the highly expressed domains (Figure S3). Comparable results were also seen for the
191 differentially expressed transcripts between the naïve vs pre-exposed and severe vs non-severe
192 comparisons, respectively (Figure S4). Remarkably, with the new whole transcript method, we observed a
193 significant decrease in clearly misassembled transcripts with, for example, an N-terminal domain at an
194 internal position (2 vs 336 misassemblies).

	Total no. contigs >= 500nt	**Maximum length (nt)**	**N50**
Original approach	6,441	10,412	2,302
Domain approach	4,691	5,003	1,088
Whole transcript approach	3,011	12,586	5,381

Table 1: Statistics for the different approaches used to assemble the *var* transcripts. *Var* assembly approaches were applied to malaria patient *ex vivo* samples (n=32) from (Wichers *et al.*, 2021) and statistics determined. Given are the total number of assembled *var* transcripts longer than 500 nt containing at least one significantly annotated *var* domain, the maximum length of the longest assembled *var* transcript in nucleotides and the N50 value, respectively. The N50 is defined as the sequence length of the shortest *var* contig, with all *var* contigs greater than or equal to this length together accounting for 50% of the total length of concatenated *var* transcript assemblies.

195
196 Overall, the new whole transcript approach performed the best on the 3D7 dataset (ENA:PRJEB31535)
197 (Wichers *et al.*, 2019), had the greatest N50, the longest *var* transcripts and produced concordant results
198 with the original analysis on the *ex vivo* samples (Wichers *et al.*, 2021). Therefore, it was selected for all
199 subsequent analyses unless specified otherwise.
200
201 **Differential expression of *var* transcripts from *ex vivo* to *in vitro* samples**
202 Of the 32 clinical isolates of *P. falciparum* from the German traveller dataset, 13 underwent one replication
203 cycle in *in vitro* culture, 10 of these underwent a second generation and one underwent a third generation
204 (Table 2). Most (9/13, 69%) isolates entering culture had a single MSP1 genotype, indicative of monoclonal
205 infections. A median of 17 million 125 bp paired-end reads, were obtained from each parasite isolate in
206 generation 1 and generation 2, the *ex vivo* samples had a greater read depth than the *in vitro* samples
207 (Table 2). Figure 3 shows a summary of the analysis performed.
208

		Generation			
		ex vivo (n=32)	Gen 1 (n=13)	Gen 2 (n=10)	Gen 3 (n=1)
Malaria exposure (n) **Naïve** **Previously exposed**		 15 17	 6 7	 4 6	 1 0
Malaria severity (n) **Severe** **Non-severe**		 8 24	 3 10	 1 9	 0 1
Number of MSP1 genotypes (number of samples)	**1**	22	9	7	1
	2	4	0	3	0
	3	5	3	0	0
	4	1	1	0	0
***P. falciparum* reads (PE*) (non-*var*) (median, IQR) (millions of reads)**		34.6 (27.0 – 36.5)	17.1 (12.9-18.0)	17.2 (12.9 -19.1)	15.1
No. non-core reads (PE*) (million of reads) (median, IQR)		5.05 (3.62 – 6.60)	1.16 (1.07 – 1.40)	1.29 (1.04– 1.58)	0.91
Number of assembled *var* contigs in a sample(>= 500nt) (Whole transcript approach) (median, IQR)		53 (44-84)	61 (38-76)	71.5 (48.25-79.5)	75
Number of assembled *var* contigs in a sample (> =1500nt and 3. sig domain annotations) (Whole transcript approach) (median, IQR)		20 (7-31)	15.5 (10-26)	15 (10.25-23.75)	18

Table 2: Summary of the dataset used in the analysis. RNA-sequencing was performed on 32 malaria infected German traveler samples (Wichers *et al.*, 2021). These 32 *ex vivo* samples were used to compare the performance of the *var* assembly approaches. Parasites from 13 of these *ex vivo* samples underwent one cycle of *in vitro* replication, 10 parasite samples were also subjected to a second cycle of replication *in vitro*, and a single parasite isolate was also analyzed after a third cycle of replication. For the *ex vivo* vs short-term *in vitro* cultivation analysis only paired samples were used. The number of assembled *var* contigs represents results per sample using the whole transcript approach, and shows either the number of assembled *var* contigs significantly annotated as *var* gene and > =500nt in length, or the number of assembled *var* transcripts identified with a length >= 1500nt and containing at least 3 significantly annotated *var* domains. *PE; paired-end reads.

To account for differences in parasite developmental stage within each sample, which are known to impact gene expression levels (Bozdech *et al.*, 2003), the proportions of life cycle stages were estimated using the mixture model approach of the original analysis (Tonkin-Hill *et al.*, 2018, Wichers *et al.*, 2021). As a complementary approach, single cell differential composition analysis (SCDC) with the Malaria Cell Atlas as a reference was also used to determine parasite age (Dong *et al.*, 2021, Howick *et al.*, 2019). SCDC and the mixture model approaches produced concordant estimates that most parasites were at ring stage in all *ex vivo* and *in vitro* samples (Figure S5a and 5b). Whilst there was no significant difference in ring stage proportions across the generations, we observed a slight increase in parasite age in the cultured samples. Overall, there were more rings and early trophozoites in the *ex vivo* samples compared to the cultured parasite samples and an increase of late trophozoite, schizont and gametocyte proportions during the culturing process (Figure S5c). The estimates produced from the mixture model approach showed high concordance with those observed by counting Giemsa stained blod smears (Figure S5d). Due to the potential confounding effect of differences in stage distribution on gene expression, we adjusted for developmental stage determined by the mixture model in all subsequent analyses.

Our new approach was applied to RNA-sequencing samples of *ex vivo* and short-term *in vitro* cultured parasites from German travellers (Wichers *et al.*, 2021). Table S2 shows the assembled *var* transcripts on a per sample basis. Interestingly, we observed SSPACE did not provide improvement in terms of extending *var* assembled contigs in 9/37 samples. We observed a significant increase in the number of assembled *var* transcripts in generation 2 parasites compared to paired generation 1 parasites ($pa_{dj} = 0.04$, paired Wilcoxon test). We observed no significant differences in the length of the assembled *var* transcripts across the generations.

231
232 Three different filtering approaches were applied in comparison to maximise the likelihood that correct
233 assemblies were taken forward for further analysis and to avoid the overinterpretation of lowly expressed
234 partial *var* transcripts (Table S3). Filtering for *var* transcripts at least 1500nt long and containing at least 3
235 significantly annotated *var* domains was the least restrictive, while the others required the presence of a
236 DBLα domain within the transcript. All three filtering approaches had the same maximum length *var*
237 transcript and similar N50 values. We observed a similar pattern of *var* transcriptional change across all
238 three filtering approaches used (described below).
239
240 Each sample's non-core reads, from which *var* assembly was performed, were mapped against a pooled
241 reference of the assembled *var* transcripts from all samples, as in Wichers *et al.*, 2021. Principal
242 component analysis (PCA) analysis was performed on the normalised *var* transcript read counts (Figure 4a
243 and b). In some patient samples, the *ex vivo* sample did not cluster closest to its paired generation 1
244 sample (patient #1, #17 and #25), suggesting there was a *var* transcriptional change in these samples
245 during the first cycle of cultivation, which was not clearly related to any technical differences in culture or
246 sequencing (explained in Methods)(Table S4). However, the rest of the samples clustered by patient
247 identity, suggesting that transition to culture had less impact than parasite origin on their *var*
248 transcriptomes. This was apparent across all three filtering approaches applied (Figure S6a and b). In line
249 with these results, *var* expression homogeneity (VEH) was investigated across the samples. The calculated
250 Bray-Curtis β diversity index showed similar clustering to that seen in the *var* transcriptome PCA, in which
251 we observed general clustering by sample identity, with the exception of the same *ex vivo* samples
252 previously identified (Figure 4a, Figure S7). This suggests that these patient samples undergo a greater *var*
253 transcriptional change when cultured compared to the other patient samples.
254

Figure 4. *Var* transcriptome analysis of *ex vivo* and short-term *in vitro* cultured parasite samples. *Var* transcripts for paired *ex vivo* (n=13), generation 1 (n=13), generation 2 (n=10) and generation 3 (n=1) were *de novo* assembled using the whole transcript approach. *Var* transcripts were filtered for those >= 1500nt in length and containing at least 3 significantly annotated *var* domains. RNA-sequencing reads were aligned to all filtered *var* transcripts assembled across all samples and expression was quantified using Salmon. **a)** PCA plot of $\log_2$ Salmon normalized read counts (adjusted for life cycle stage, derived from the mixture model approach). Points are coloured by their generation (*ex vivo*: purple, generation 1: red, generation 2: green, and generation 3: blue) and labelled by their patient identity. **b)** PCA plot of $\log_2$ Salmon normalized read counts (adjusted for life cycle stage, derived from the mixture model approach)for *ex vivo* (blue) and paired generation 1 (red) samples. Points are labelled by their patient identity. **c)** Volcano plot showing extent and significance of up- or down-regulation of *var* gene expression in *ex vivo* (n=13) compared with paired generation 1 cultured parasites (n=13) (red and blue: $P < 0.05$ after Benjamini-Hochberg adjustment for FDR, red and green: absolute $\log_2$ fold change $\log_2$FC in expression >= 2). Transcripts with a $\log_2$FC > = 2 represent those upregulated in generation 1 parasites. Transcripts with a $\log_2$FC <= -2 represent those downregulated in generation 1 parasites. **d)** Volcano plot showing extent and significance of up- or down-regulation of *var* gene expression in *ex vivo* (n=10) compared with paired generation 2 cultured parasites (n=10) (green: absolute $\log_2$ fold change in expression >= 2). Transcripts with a $\log_2$FC >= 2 represent those upregulated in generation 2 parasites. Transcripts with a $\log_2$FC <= -2 represent those downregulated in generation 2 parasites. **e)** *var2csa* expression through short-term *in vitro* cultivation. All significantly annotated *var2csa* transcripts had their $\log_2$ Salmon normalised count summed. Significant differences in expression levels between generations were assessed using a paired Wilcoxon test and adjusted using the Benjamini-Hochberg method. Numbers above the boxplots represent significant differences observed (FDR <=0.05). Coloured lines connect paired patient samples through the generations. **f)** Volcano plot showing extent and significance of up- or down-regulation of *var* gene expression in generation 1 (n=10) compared with paired generation 2 cultured parasites (n=10) (green: absolute $\log_2$ fold change $\log_2$FC >=2). Transcripts with a $\log_2$FC >= 2 represent those upregulated in generation 2 parasites. Transcripts with a $\log_2$FC <= -2 represent those downregulated in generation 2 parasites. **g)** *Var* transcript expression differences for the differentially expressed *var* transcripts in the paired *ex vivo* (n=13) vs generation 1 (n=13) parasite sample analysis. Box plots show $\log_2$-transformed normalized Salmon read counts adjusted for life cycle stage estimates (derived from the mixture model approach) across the generations (blue: *ex vivo*, orange, generation 1: green, generation 2, and red: generation 3). Normalised counts had 0.5 added prior to $\log_2$ transformation.

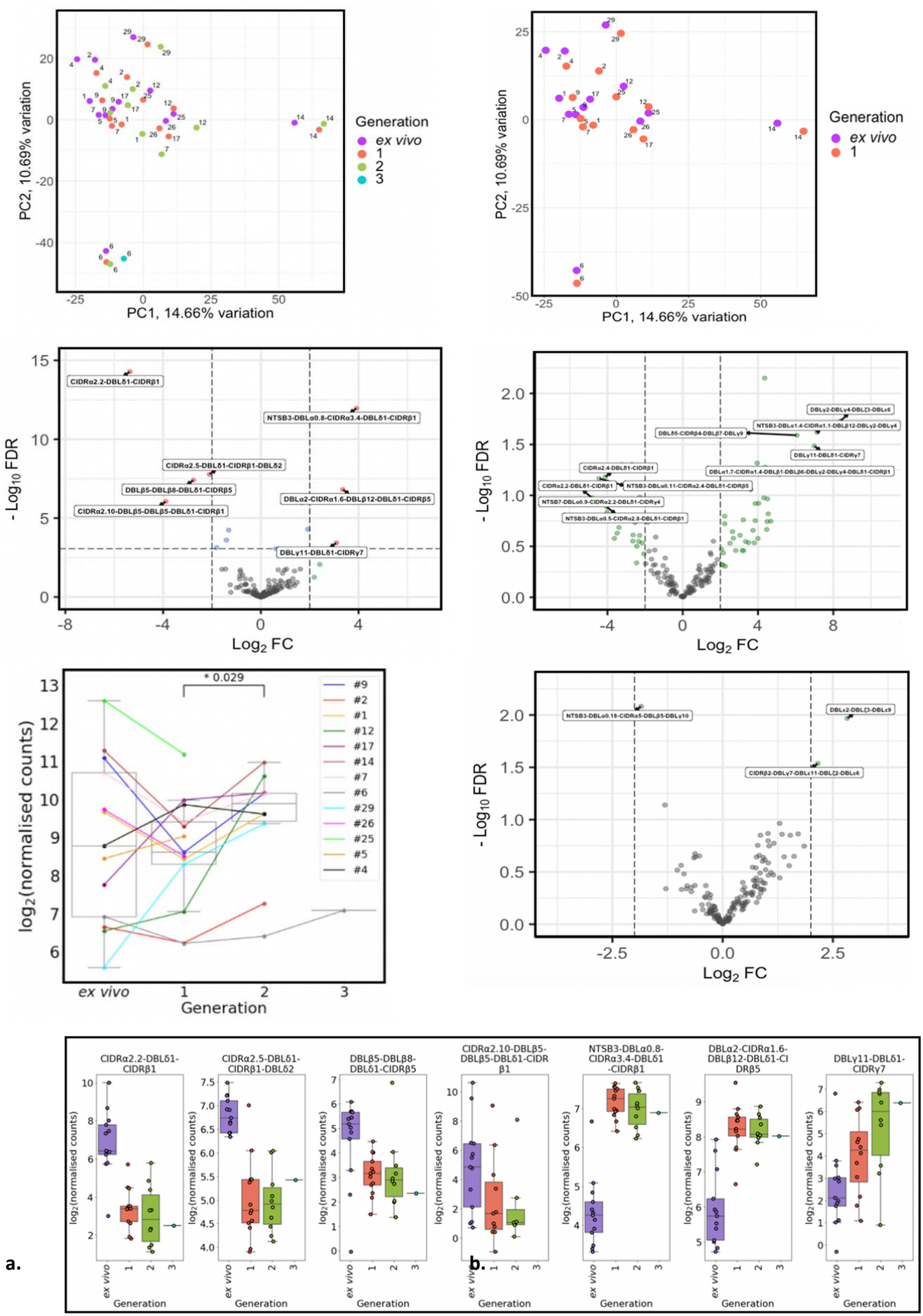
PC2, 10.69% variation
PC1, 14.66% variation
Generation
ex vivo
1
2
3
- Log10 FDR
Log2 FC
CIDRα2.2-DBLδ1-CIDRβ1
NTSB3-DBLα0.8-CIDRα3.4-DBLδ1-CIDRβ1
CIDRα2.5-DBLδ1-CIDRβ1-DBLδ2
DBLβ5-DBLβ8-DBLδ1-CIDRβ5
DBLα2-CIDRα1.6-DBLβ12-DBLδ1-CIDRβ5
CIDRα2.10-DBLβ5-DBLβ5-DBLδ1-CIDRβ1
DBLγ11-DBLδ1-CIDRγ7
log2(normalised counts)
* 0.029
#9
#2
#1
#12
#17
#14
#7
#6
#29
#26
#25
#5
#4
a.
b.

256 Seven *var* transcripts were found to be significantly differentially expressed in the *ex vivo* vs generation 1
257 comparison (Figure 4c). We observed no significant differences in the expression of conserved *var* gene
258 variants, *var1-IT (*p_{adj} = 0.61*,* paired Wilcoxon test)*, var1-3D7* (p_{adj} =0.93*,* paired Wilcoxon test) and *var2csa*
259 (p_{adj} =0.54, paired Wilcoxon test*)* between paired *ex vivo* and generation 1 parasites*.* This represents a
260 relatively small number of *var* transcripts differentially expressed out of the 455 assembled *var* transcripts.
261 The comparison between generation 2 and *ex vivo* had a smaller number of samples, however we
262 observed a similar pattern, in terms of the differentially expressed transcripts, to that of the *ex vivo* vs
263 generation 1 comparison (Figure 4d). *Var2csa* was significantly differentially expressed between
264 generation 1 and generation 2 parasites (p_{adj} = 0.029, paired Wilcoxon test)(Figure 4e). No other *var*
265 transcripts were significantly differentially expressed in the comparison between generation 1 vs
266 generation 2 parasite samples (Figure 4f), suggesting the *var* transcriptomes of these two generations are
267 highly similar and that any major changes in *var* expression occur at the start of the cultivation. The
268 log_2Fold change (log_2FC) observed in the *ex vivo* vs generation 2 comparison were greater than in the *ex*
269 *vivo* vs generation 1 comparison, suggesting that the transcriptional changes initiated in the first cycle of
270 cultivation, are reinforced during ongoing cultivation. However, *var2csa* expression appeared to decrease
271 in some paired samples during the first cycle of cultivation (Figure 4e). Similar results were observed across
272 all filtering approaches used (Figure S6c, d, e and f). Overall, the *var* transcript differential expression
273 analysis shows relatively small changes in *var* expression from *ex vivo* to culture. These small changes
274 might be explained by the loss of selection pressure which occurs *in vivo*.
275
276 Of the 7 differentially expressed transcripts in the *ex vivo* vs generation 1 comparison, the four
277 downregulated *var* transcripts in the generation 1 samples included three encoding CD36 binding PfEMP1
278 proteins (CIDRα2.2- DBLδ1-CIDRβ1, CIDRα2.5-DBLδ1-CIDRβ1-DBLδ2, CIDRα2.10-DBLβ5-DBLβ5-DBLδ1-
279 CIDRβ1). The three transcripts upregulated in generation 1 encode the CD36-binder NTSB3-DBLα0.8-
280 CIDRα3.4-DBLδ1-CIDRβ1, the EPCR-binder DBLα2-CIDRα1.6-DBLβ12-DBLδ1-CIDRβ5 and a C-terminal
281 fragment with unknown N-terminus and associated binding phenotype (DBLγ11-DBLδ1-CIDRγ7)(Figure
282 4g). To verify that the differentially expressed transcripts were not due to differential growth of multiple
283 parasite clones within a sample, differential expression analysis of *var* gene expression between *ex vivo*
284 and generation 1 samples was repeated in the subset of samples with only a single MSP1 genotype (Figure
285 S8a). There was a high correlation (Spearman's rank correlation = 0.87) between the log_2FC values of these
286 samples with those of all samples (Figure S8b). This suggests the differentially expressed *var* transcripts are
287 not due to multiple *Plasmodium* genotypes being present or inadvertent selective culture of a single
288 parasite clone from a polyclonal infection.
289
290 **Differential expression of *var* domains from *ex vivo* to *in vitro* samples**
291 Next, we performed differential expression analysis on the level of encoded PfEMP1 domain subtypes, as
292 done in previous studies, which can be associated with *var* gene groups and receptor binding phenotypes
293 (Tonkin-Hill *et al.*, 2018, Wichers *et al.*, 2021). Similar to the transcript level analysis, PCA on *var* domain
294 expression (Figure 5a) showed some patients' *ex vivo* samples clustering away from their respective
295 generation 1 sample (patient #1, #2, #4, #17, #25 and #12), again indicating a greater *var* transcriptional
296 change relative to the other samples during the first cycle of cultivation.

a.

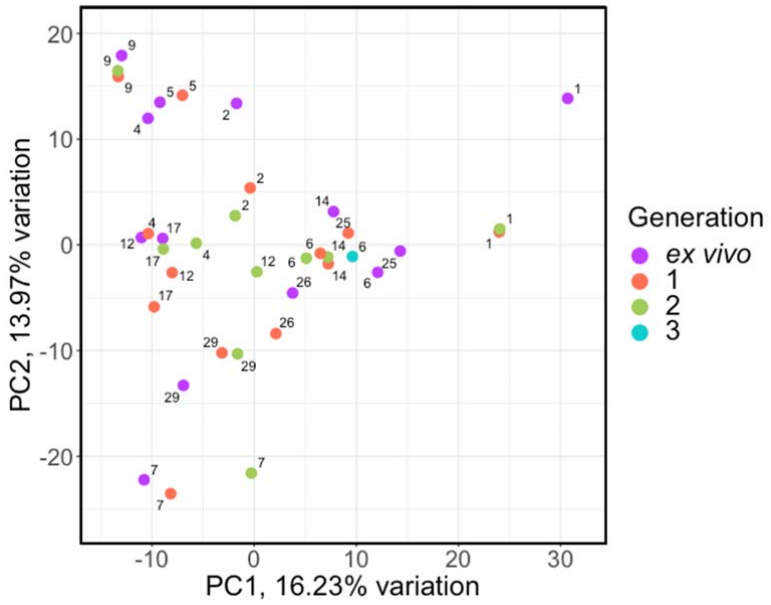

b.

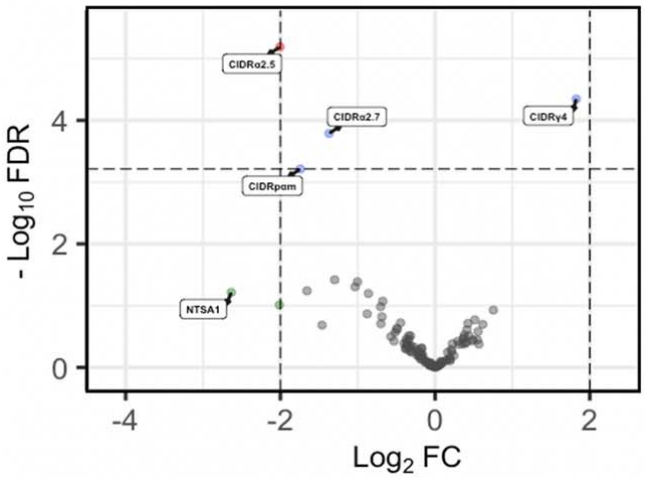

c.

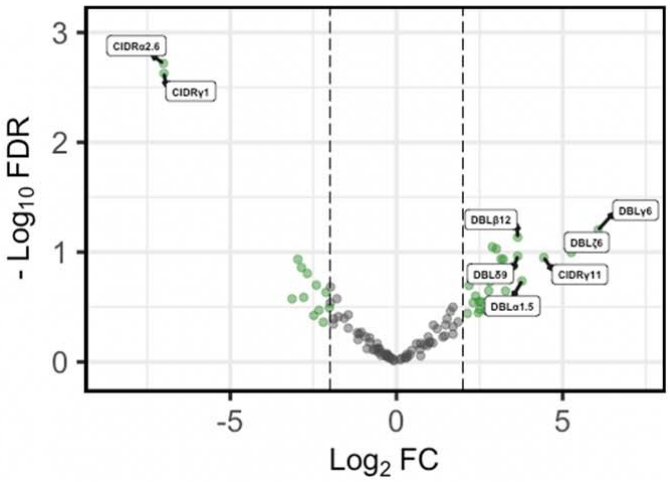

Figure 5: *Var* domain transcriptome analysis through short-term *in vitro* culture. *Var* transcripts for paired *ex vivo* (n=13), generation 1 (n=13), generation 2 (n=10) and generation 3 (n=1) were *de novo* assembled using the whole transcript approach. *Var* transcripts were filtered for those >= 1500nt in length and containing at least 3 significantly annotated *var* domains. Transcripts were annotated using HMM models built on the Rask et al., 2010 dataset (Rask *et al.*, 2010). When annotating the whole transcript, the most significant alignment was taken as the best annotation for each region of the assembled transcript (e-value cut off 1e-5). Multiple annotations were allowed on the transcript if they were not overlapping, determined using cath-resolve-hits. *Var* domain expression was quantified using FeatureCounts and the domain counts aggregated **a)** PCA plot of log_2 normalized read counts (adjusted for life cycle stage, derived from the mixture model approach). Points are coloured by their generation (*ex vivo*; purple, generation 1; red, generation 2; green and generation 3; blue) and labelled by their patient identity **b)** Volcano plot showing extent and significance of up- or down-regulation of *var* domain expression in *ex vivo* (n=13) compared with paired generation 1 cultured parasites (n=13) (red and blue, $P < 0.05$ after Benjamini-Hochberg adjustment for FDR; red and green, absolute log_2 fold change log_2FC in expression >= 2). Domains with a log_2FC > = 2 represent those upregulated in generation 1 parasites. Domains with a log_2FC <= -2 represent those downregulated in generation 1 parasites **c)** Volcano plot showing extent and significance of up- or down-regulation of *var* domain expression in *ex vivo* (n=10) compared with paired generation 2 cultured parasites (n=10) (green, absolute log_2 fold change log_2FC in expression >= 2). Domains with a log_2FC >= 2 represent those upregulated in generation 2 parasites. Domains with a log_2FC <= -2 represent those downregulated in generation 2 parasites. Differential expression analysis was performed using DESeq2 (adjusted for life cycle stage, derived from the mixture model approach).

298 In the generation 1 vs *ex vivo* comparison, a single domain was significantly differentially expressed,
299 CIDRα2.5 associated with B-type PfEMP1 proteins and CD36-binding (Figure 5b). In the generation 2 vs *ex*
300 *vivo* comparison, there were no domains significantly differentially expressed, however we observed large
301 $\log_2$FC values in similar domains to those changing most in the *ex vivo* vs generation 1 comparison (Figure
302 5c). No differentially expressed domains were found in the generation 1 vs generation 2 comparison.
303
304 **Cultured parasites as surrogates for assessing the *in vivo var* transcriptome**
305 Parasite isolates from malaria patients are often studied in short-term culture to investigate relationships
306 between parasite factors such as *var* gene expression, cytoadhesion phenotype, and host clinical or
307 immunological status. To understand how culture-induced changes in *var* gene expression may impact the
308 interpretation of such analyses, we performed differential expression analysis comparing parasite isolates
309 from naïve (n=6) versus previously-exposed (n=7) patients with paired *ex vivo* and generation 1 samples.
310 This was performed using the 'all sample analysis' approach (Figure 3) with the same reference of
311 assembled *var* transcripts used for the *ex vivo* and generation 1 analysis. There were 75 differentially
312 expressed transcripts in the *ex vivo* samples, but only 18 differentially expressed transcripts in the
313 generation 1 analysis (Figure S9a and S9b). The transcripts that were differentially expressed in the
314 generation 1 samples were similar to those found in the *ex vivo* samples, but there were smaller fold
315 change values in the generation 1 analysis. However, one transcript that was significantly upregulated in
316 naïve patients in the *ex vivo* samples was found to be downregulated in the generation 1 sample analysis
317 (encoding CD36-binding NTSB3-DBLα0.5-CIDRα2.3-DBLδ1-CIDRß1). The differential selection pressure
318 between previously exposed and malaria-naïve patients is removed during culture. Our results suggest the
319 removal of this pressure results in the *var* transcriptomes of different parasites becoming more similar to
320 each other, independent of their original *in vivo* transcriptional state.
321
322 **Per patient *var* transcript analysis**
323 Different parasite isolates have different *var* genomic repertoires, whilst differential expression analysis
324 assumes all samples could express the same transcripts. Prior to differential expression analysis, a
325 combined reference is created from the assemblies in all samples and read mapping is performed (Figure
326 3, 'all sample analysis'). This allows reads from one sample to map to *var* gene assemblies from a different
327 sample, but this mapping may not always correctly represent the true origin of each read. We sought to
328 address these limitations by analysing *var* gene expression at an individual subject level, where we
329 confirmed the MSP1 genotypes and alleles were still present after short-term *in vitro* cultivation. There are
330 about 60 *var* genes in each *P. falciparum* genome, however, each individual parasite expresses only a
331 single *var* gene at any given time. To investigate whether dominant *var* gene expression changes through
332 *in vitro* culture, rank analysis of *var* transcript expression was performed (Figure S10). In most cases the
333 dominant *var* transcripts were concordant between *ex vivo* and *in vitro* cultured samples from the same
334 patient, with a single dominant *var* transcript. This suggests the parasites were behaving clonally, a
335 phenomenon described previously (Bachmann *et al.*, 2011). However, we observed a change in the
336 dominant *var* gene being expressed through culture in isolates from patients #6, #17 and #26. Except #17,
337 these were not the samples identified in the transcript and domain analysis when all samples' *var* gene
338 assemblies were combined and expression quantified. Changes in the dominant *var* gene expression were
339 also observed in the DBLα-tag data for these patients (described below). In patients #7, #1 and #14, the
340 top expressed *var* gene remained the same, however we observed a change in the ranking of other highly
341 expressed *var* genes in the cultured samples compared to the *ex vivo.* This suggests some parasites in
342 these samples underwent *var* gene switching, and in the samples where the dominant *var* gene changed, a
343 fast-switching event might have occurred (Bachmann *et al.*, 2011). Interestingly, in patient #26 we
344 observed a switch from a dominant group A *var* gene to a group B and C *var* gene. This finding was also
345 observed in the DBLα-tag analysis (results below). A similar finding was seen in patient #7. In the *ex vivo*
346 sample, the second most expressed *var* transcript was a group A transcript. However, in the cultured

347 samples expression of this transcript was reduced and we observed an increase in the expression of group
348 B and C *var* transcripts. A similar pattern was observed in the DBLα-tag analysis for patient #7, whereby the
349 expression of a group A transcript was reduced during the first cycle of cultivation. The dominant *var* gene
350 did not change in the other patient samples and the ranking of *var* gene expression remained similar. This
351 again suggests that some patient samples underwent a larger *var* transcriptional change when cultured
352 compared to the other patient samples, and that culturing parasites can lead to an unpredictable *var*
353 transcriptional change.
354
355 In line with these results, VEH on a per patient basis showed in some patients a clear change, with the *ex*
356 *vivo* sample diversity curve distinct from those of *in vitro* generation 1 and generation 2 samples (patient
357 #4, #1 and #2) (Figure S11). Similarly, in other patient samples, we observed a clear difference in the curves
358 of *ex vivo* and generation 1 samples (patient #25 and #26, both from malaria-naïve severe malaria
359 patients). Some of these samples (#1 and #26, both from malaria-naïve severe malaria patients) also
360 showed changes in their dominant *var* gene expression during culture, taken together indicating much
361 greater *var* transcriptional changes *in vitro* compared to the other samples.
362
363 ***Var* group expression analysis**
364 A previous study found group A *var* genes to have a rapid transcriptional decline in culture compared to
365 group B *var* genes, however another study found a decrease in both group A and group B *var* genes in
366 culture (Zhang *et al.*, 2011, Peters *et al.*, 2007). These studies were limited as the *var* type was determined
367 by analysing the sequence diversity of DBLα domains, and by quantitative PCR (qPCR) methodology which
368 restricts analysis to quantification of known/conserved sequences. Due to these results, the expression of
369 group A *var* genes vs. group B and C *var* genes was investigated using a paired analysis on all the DBLα
370 (DBLα1 vs DBLα0 and DBLα2) and NTS (NTSA vs NTSB) sequences assembled from *ex vivo* samples and
371 across multiple generations in culture. A linear model was created with group A expression as the
372 explanatory variable, the generation and life cycle stage as independent variables and the patient
373 information included as a random effect. The same was performed using group B and C expression levels.
374
375 In both approaches (DBLα and NTS) we found no significant changes in total group A or group B and C *var*
376 gene expression levels (Figure 6). We observed high levels of group B and C *var* gene expression compared
377 to group A in all patients, both in the *ex vivo* samples and the *in vitro* samples. In some patients we
378 observed a decrease in group A *var* genes from *ex vivo* to generation 1 (patients #5, #2, #26, #12, #6, #9, #1
379 and #17)(Figure 6a), however in all but four patients (patient #1, #5, #6 and #2) the levels of group B and C
380 *var* genes remained consistently high from *ex vivo* to generation 1 (Figure 6b). Interestingly, patients #17
381 and #6 also had a change in the dominant *var* gene expression through culture. Taken together with the
382 preceding results, it appears that observed differences in *var* transcript expression occurring with
383 transition to short-term culture are not due to modulation of recognised *var* classes, but due to differences
384 in expression of particular *var* transcripts.
385

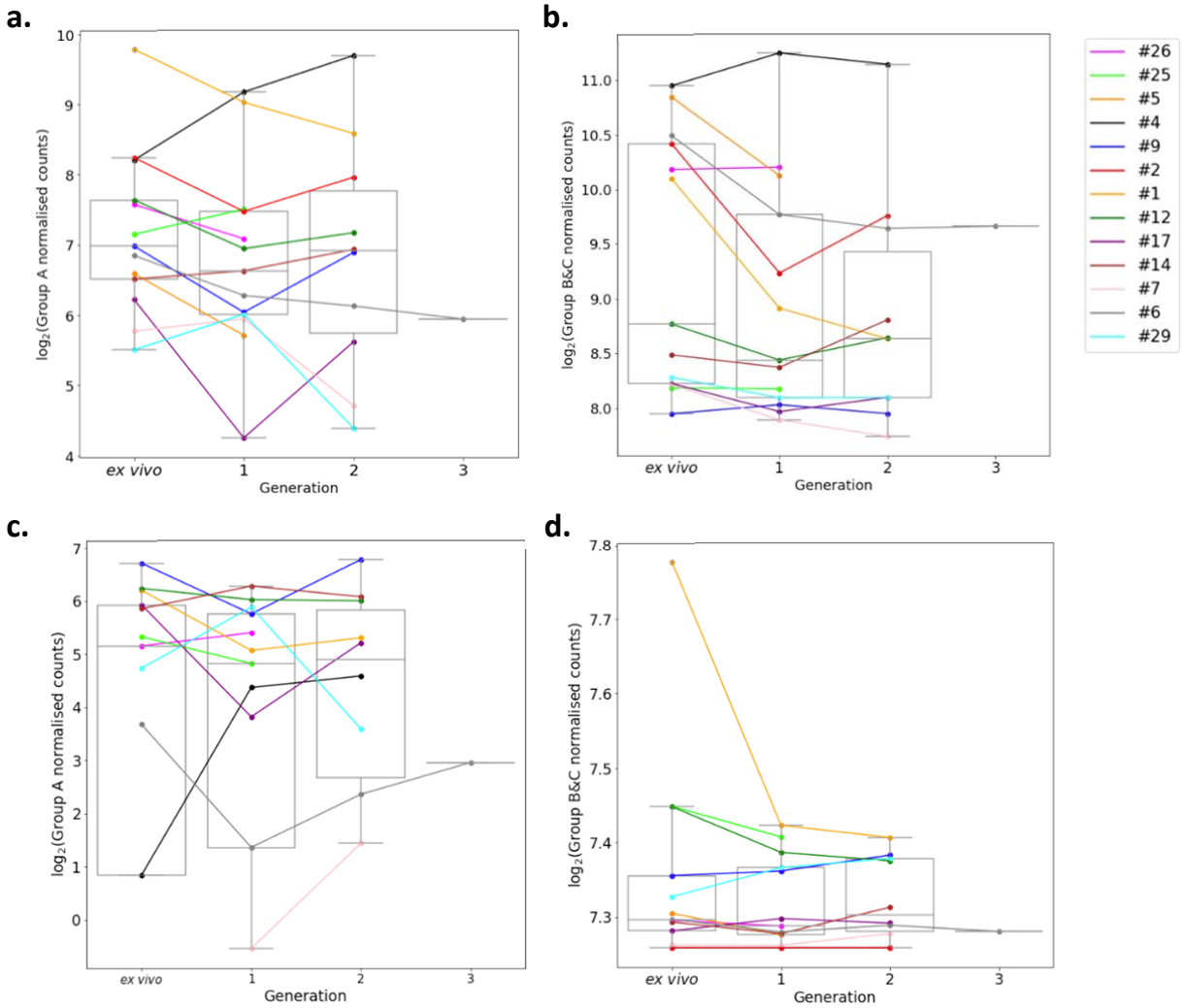

Figure 6. *Var* group expression analysis through short-term *in vitro* culture. The DBLα domain sequence for each transcript was determined and for each patient a reference of all assembled DBLα domains combined. Group A *var* genes encode DBLα1, group B encode DBLα2 and groups B and C encode DBLα0. Domains were grouped by type and their expression summed. The relevant sample's non-core reads were mapped to this using Salmon and DBLα expression quantified. DESeq2 normalisation was performed, with patient identity and life cycle stage proportions included as covariates. A similar approach was repeated for NTS domains. Group A *var* genes encode NTSA compared to group B and C *var* genes which encode NTSB. Boxplots show $\log_2$ normalised Salmon read counts for **a)** group A *var* gene expression through cultured generations assessed using the DBLα domain sequences **b)** group B and C *var* gene expression through cultured generations assessed using the DBLα domain sequences **c)** group A *var* gene expression through cultured generations assessed using the NTS domain sequences **d)** group B and C *var* gene expression through cultured generations assessed using the NTS domain sequences. Different coloured lines connect paired patient samples through the generations (*ex vivo* (n=13) and generation 1 (n=13) samples vs *ex vivo* (n=9) and generation 1 (n=9)).

386 **<u>Quantification of total *var* gene expression</u>**
387 We observed a trend of decreasing total *var* gene expression between generations irrespective of the
388 assembler used in the analysis (Figure S12). A similar trend is seen with the LARSFADIG count, which is
389 commonly used as a proxy for the number of different *var* genes expressed (Otto *et al.*, 2019). A linear
390 model was created (using only paired samples from *ex vivo* and generation 1)(Supplementary file 1) with
391 proportion of total gene expression dedicated to *var* gene expression as the explanatory variable, the
392 generation and life cycle stage as independent variables and the patient information included as a random
393 effect. This model showed no significant differences between generations, suggesting that differences
394 observed in the raw data may be a consequence of small changes in developmental stage distribution in
395 culture.
396
397

398 ***Var* expression profiling by DBLα-tag sequencing**
399 Deep sequencing of RT-PCR-amplified DBLα expressed sequence tags (ESTs) combined with prediction of
400 the associated transcripts and their encoded domains using the Varia tool (Mackenzie *et al.*, 2022) was
401 performed, as in the original analysis, to supplement the RNA-sequencing analysis. The raw Varia output
402 file is given in Supplementary file 2. Overall, we found a high agreement between the detected DBLα-tag
403 sequences and the *de novo* assembled *var* transcripts. Around 94% (median) of all unique DBLα-tag
404 sequences detected with >10 reads were found in the RNA-sequencing approach. This is an improvement
405 on the original approach, in which a median of 82.6% was found (Wichers *et al.*, 2021). To allow for a fair
406 comparison of the >10 reads threshold used in the DBLα-tag approach, the upper 75th percentile of the
407 RNA-sequencing-assembled DBLα domains were analysed. A median of 73.4% of the upper 75th percentile
408 of the assembled DBLα domains were found in the DBLα-tag approach. This is a lower median percentage
409 than that found in the original analysis (81.8%) and suggests the new approach might be better at
410 capturing all expressed DBLα domains.
411
412 The new whole transcript assembly approach also had high consistency with the domain annotations
413 predicted from Varia. Varia predicts *var* sequences and domain annotations based on short sequence tags,
414 using a database of previously defined *var* sequences and annotations (Mackenzie *et al.*, 2022). A median
415 of 85% was observed for the DBLα annotations identified from the DBLα-tag approach that were found in
416 the RNA-sequencing approach. A median of 73% was observed for the DBLα-CIDR domain annotations
417 identified from the DBLα-tag approach that were found in the RNA-sequencing approach. We also
418 observed consistent results with the per patient analysis, in terms of changes in the dominant *var* gene
419 expression (described above)(Supplementary file 2). In line with the RNA-sequencing data, the DBLα-tag
420 approach revealed no significant differences in Group A and Group B and C groups during short-term
421 culture, further highlighting the agreement of both methods (Figure S13).
422
423 **Core gene differential expression**
424 Given the modest changes in *var* gene expression repertoire upon culture we wanted to investigate the
425 extent of any accompanying changes in the core parasite transcriptome. PCA was performed on core gene
426 (*var, rif, stevor, surf* and rRNA genes removed) expression, adjusted for life cycle stage. We observed
427 distinct clustering of *ex vivo*, generation 1, and generation 2 samples, with patient identity having much
428 less influence (Figure 7a). There was also a change from the heterogeneity between the *ex vivo* samples to
429 more uniform clustering of the generation 1 samples (Figure 7b), suggesting that during the first cycle of
430 cultivation the core transcriptomes of different parasite isolates become more alike. The effect of sample
431 type on the core gene PCA was much clearer than on the *var* transcript PCA (Figure 4a), suggesting the
432 core gene transcriptome underwent a greater change relative to the *var* transcriptome upon transition to
433 culture.
434

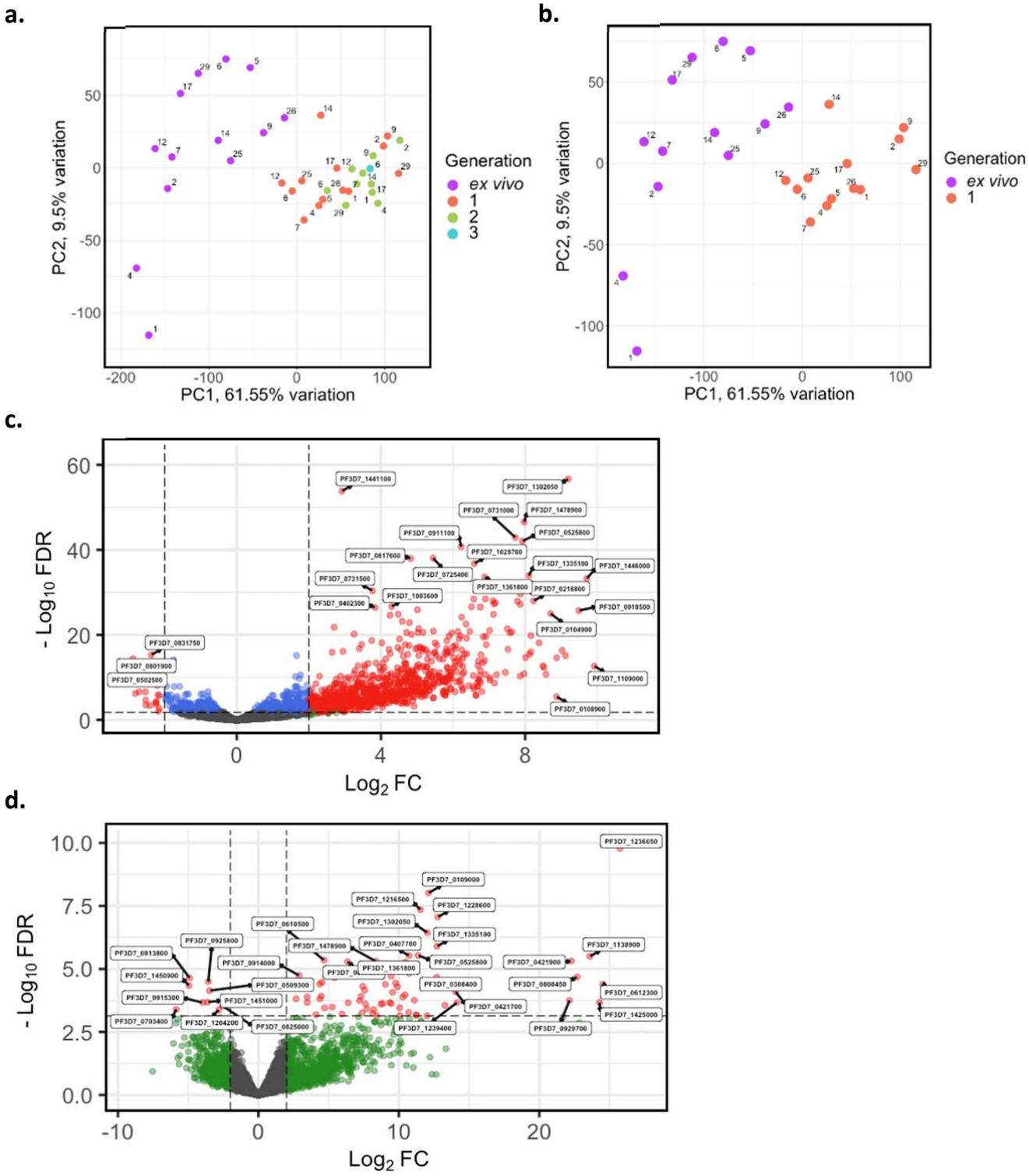

Figure 7: Core gene transcriptome analysis of *ex vivo* and short-term *in vitro* cultured samples. Core gene expression was assessed for paired *ex vivo* (n=13), generation 1 (n=13), generation 2 (n=10) and generation 3 (n=1) parasite samples. Subread align was used, as in the original analysis, to align the reads to the human genome and *P. falciparum* 3D7 genome, *with var, rif, stevor, surf* and *rRNA* genes removed. HTSeq count was used to quantify gene counts. **a)** PCA plot of $\log_2$ normalized read counts. Points are coloured by their generation (*ex vivo*: purple, generation 1: red, generation 2: green, and generation 3: blue) and labelled by their patient identity. **b)** PCA plot of $\log_2$ normalized read counts for *ex vivo* (purple) and paired generation 1 (red) samples. Points are labelled by their patient identity. **c)** Volcano plot showing extent and significance of up- or down-regulation of core gene expression in *ex vivo* (n=13) compared with paired generation 1 cultured parasites (n=13) (red and blue: $P < 0.05$ after Benjamini-Hochberg adjustment for FDR, red and green: absolute $\log_2$ fold change $\log_2$FC in expression >= 2). Genes with a $\log_2$FC > = 2 represent those upregulated in generation 1 parasites. Genes with a $\log_2$FC <= -2 represent those downregulated in generation 1 parasites. **d)** Volcano plot showing extent and significance of up- or down-regulation of core gene expression in *ex vivo* (n=10) compared with paired generation 2 cultured parasites (n=10) (red: $P < 0.05$ after Benjamini-Hochberg adjustment for FDR, red and green: absolute $\log_2$ fold change $\log_2$FC in expression >= 2). Genes with a $\log_2$FC >= 2 represent those upregulated in generation 2 parasites. Genes with a $\log_2$FC <= -2 represent those downregulated in generation 2 parasites. Normalized read counts of the core gene analysis were adjusted for life cycle stage, derived from the mixture model approach.

436 In total, 920 core genes (19% of the core transcriptome) were found to be differentially expressed after
437 adjusting for life cycle stages using the mixture model approach between *ex vivo and* generation 1 samples
438 (Supplementary file 3). The majority were upregulated, indicating a substantial transcriptional change
439 during the first cycle of *in vitro* cultivation (Figure 7c). 74 genes were found to be upregulated in
440 generation 2 when compared to the *ex vivo* samples, many with $\log_2$FC greater than those in the *ex vivo* vs
441 generation 1 comparison (Figure 7d). No genes were found to be significantly differentially expressed
442 between generation 1 and generation 2. However, five genes had a $\log_2$FC >= 2 and were all upregulated in
443 generation 2 compared to generation 1. Interestingly, the gene with the greatest fold change, encoding
444 ROM3 (PF3D7_0828000), was also found to be significantly downregulated in generation 1 parasites in the
445 *ex vivo* vs generation 1 analysis. The other four genes were also found to be non-significantly
446 downregulated in generation 1 parasites in the *ex vivo* vs generation 1 analysis. Similar to the *var*
447 transcriptome analysis, this suggests changes in gene expression during the first cycle of cultivation are the
448 greatest compared to the other cycles.
449
450 The most significantly upregulated genes (in terms of fold change) in generation 1 contained several small
451 nuclear RNAs, splicesomal RNAs and non-coding RNAs (ncRNAs). 16 ncRNAs were found upregulated in
452 generation 1, with several RNA-associated proteins having large fold changes ($\log_2$FC > 7) Significant gene
453 ontology (GO) terms and Kyoto encyclopedia of genes and genomes (KEGG) pathways for the core genes
454 upregulated in generation 1 included 'entry into host', 'movement into host' and 'cytoskeletal
455 organisation' suggesting the parasites undergo a change in invasion efficiency, which is connected to the
456 cytoskeleton, during their first cycle of *in vitro* cultivation (Figure S14). We observed eight AP2
457 transcription factors upregulated in generation 1 (PF3D7_0404100/AP2-SP2, PF3D7_0604100/SIP2,
458 PF3D7_0611200/AP2-EXP2, PF3D7_0613800, PF3D7_0802100/AP2-LT, PF3D7_1143100/AP2-O,
459 PF3D7_1239200, PF3D7_1456000/AP2-HC) with no AP2 transcription factors found to be downregulated in
460 generation 1. To confirm the core gene expression changes identified were not due to the increase in
461 parasite age during culture, as indicated by upregulation of many schizont-related genes, core gene
462 differential expression analysis was performed on paired *ex vivo* and generation 1 samples that contained
463 no schizonts or gametocytes in generation 1. The same genes were identified as significantly differentially
464 expressed with a Spearman's rank correlation of 0.99 for the $\log_2$FC correlation between this restricted
465 sample approach and those produced using all samples (Figure S15).
466
467 **<u>Cultured parasites as surrogates for assessing the *in vivo* core gene transcriptome</u>**
468 Due to the high number of core genes found to be significantly differentially expressed in the *ex vivo* vs
469 generation 1 comparison, we further investigated the suitability of cultured parasites being used as
470 surrogates for assessing the *in vivo* core gene transcriptome. We performed differential expression analysis
471 comparing parasite isolates from naïve (n=6) vs pre-exposed (n=7) patients, between their *ex vivo* samples
472 and then separately between their paired generation 1 samples. Interestingly, when using the *ex vivo*
473 samples, we observed 206 core genes significantly upregulated in naïve patients compared to pre-exposed
474 patients (Figure S16a). Conversely, we observed no differentially expressed genes in the naïve vs pre-
475 exposed analysis of the paired generation 1 samples (Figure S16b). Taken together, this suggests one cycle
476 of cultivation shifts the core transcriptomes of parasites to be more alike each other, diminishing
477 inferences about parasite biology *in vivo*.
478
479 **<u>Discussion</u>**
480 Multiple lines of evidence point to PfEMP1 as a major determinant of malaria pathogenesis, but previous
481 approaches for characterising *var* expression profiles in field samples have limited *in vivo* studies of
482 PfEMP1 function, regulation, and association with clinical symptoms (Tarr *et al.*, 2018, Lee *et al.*, 2018,
483 Warimwe *et al.*, 2013, Rorick *et al.*, 2013, Zhang *et al.*, 2011, Taylor *et al.*, 2002). A more recent approach,
484 based on RNA-sequencing, overcame many of the limitations imposed by the previous primer-based

485 methods (Tonkin-Hill *et al.*, 2018, Wichers *et al.*, 2021). However, depending on the expression level and
486 sequencing depth, *var* transcripts were found to be fragmented and only a partial reconstruction of the *var*
487 transcriptome was achieved (Tonkin-Hill *et al.*, 2018, Wichers *et al.*, 2021, Andrade *et al.*, 2020, Guillochon
488 *et al.*, 2022, Yamagishi *et al.*, 2014). The present study developed a novel approach for *var* gene assembly
489 and quantification that overcomes many of these limitations.
490
491 Our new approach used the most geographically diverse reference of *var* gene sequences to date, which
492 improved the identification of reads derived from *var* transcripts. This is crucial when analysing patient
493 samples with low parasitaemia where *var* transcripts are hard to assemble due to their low abundancy
494 (Guillochon *et al.*, 2022). Our approach has wide utility due to stable performance on both laboratory-
495 adapted and clinical samples. Concordance in the different *var* expression profiling approaches (RNA-
496 sequencing and DBLα-tag) increased using the new approach by 11.4%, when compared to the original
497 approach (94% in the whole transcript approach compared to 82.6% in Wichers *et al.*, 2021. This suggests
498 the new approach provides a more reliable and robust method for characterising *var* genes.
499
500 Having a low number of long contigs is desirable in any *de novo* assembly. This reflects a continuous
501 assembly, as opposed to a highly fragmented one where polymorphic and repeat regions could not be
502 resolved (Lischer & Shimizu, 2017). An excessive number of contigs cannot be reasonably handled
503 computationally and results from a high level of ambiguity in the assembly (Yang *et al.*, 2012). We
504 observed a greater than 50% reduction in the number of contigs produced in our new approach, which
505 also had a 21% increase in the maximum length of the assembled *var* transcripts, when compared to the
506 original approach. It doubled the assembly continuity and assembled an average 13% more of the *var*
507 transcripts. This was particularly apparent in the N-terminal region, which has often been poorly
508 characterised by existing approaches. The original approach failed to assemble the N-terminal region in
509 58% of the samples, compared to just 4% in the new approach with assembly consistently achieved with an
510 accuracy > 90%. This is important because the N-terminal region is known to contribute to the adhesion
511 phenotypes of most PfEMP1s.
512
513 The new approach allows for *var* transcript reconstruction across a range of expression levels, which is
514 required when characterising *var* transcripts from multi-clonal infections. Assembly completeness of the
515 lowly expressed *var* genes increased five-fold using the new approach. Biases towards certain parasite
516 stages have been observed in non-severe and severe malaria cases, so it is valuable to assemble the *var*
517 transcripts from different life cycle stages (Tonkin-Hill *et al.*, 2018). Our new approach is not limited by
518 parasite stage. It was able to assemble the whole *var* transcript, in a single contig, at later stages in the *P.*
519 *falciparum* 3D7 intra-erythrocytic cycle, something previously unachievable. The new approach allows for a
520 more accurate and complete picture of the *var* transcriptome. It provides new perspectives for relating *var*
521 expression to regulation, co-expression, epigenetics and malaria pathogenesis. It has huge applicability, for
522 example analysis of patient samples with different clinical outcomes and longitudinal tracking of infections
523 *in vivo*. It represents a crucial improvement for quantifying the *var* transcriptome. In this work, the
524 improved approach for *var* gene assembly and quantification was used to characterise *var* gene expression
525 during transition from *in vivo* to short-term culture.
526
527 Studies have been performed investigating differences between long-term laboratory-adapted clones and
528 clinical isolates, with hundreds of genes found to be differentially expressed (Hoo *et al.*, 2019, Tarr *et al.*,
529 2018, Mackinnon *et al.*, 2009). Surprisingly, studies investigating the impact of short-term culture on
530 parasites are extremely limited, despite it being commonly undertaken for making inferences about the *in*
531 *vivo* transcriptome (Vignali *et al.*, 2011). Using the new *var* assembly approach, we found that *var* gene
532 expression remains relatively stable during transition to culture, with only a small number of differentially
533 expressed transcripts across the whole dataset. These included *var2csa*, which had increased expression
534 from generation 1 to generation 2. It has previously been suggested that long-term cultured parasites

535 converge to expressing *var2csa*, but our findings suggest this begins within two cycles of cultivation (Zhang
536 *et al.*, 2022, Mok *et al.*, 2008). Switching to *var2csa* has been shown to be favourable and is suggested to
537 be the default *var* gene of choice upon perturbation to *var* specific heterochromatin (Ukaegbu *et al.*,
538 2015). These studies also suggested *var2csa* has a unique role in *var* gene switching and our results are
539 consistent with the role of *var2csa* as the dominant 'sink node' (Zhang *et al.*, 2022, Ukaegbu *et al.*, 2015,
540 Ukaegbu *et al.*, 2014, Mok *et al.*, 2008). A previous study suggested *in vitro* cultivation of controlled human
541 malaria infection samples resulted in dramatic changes in *var* gene expression (Lavstsen *et al.*, 2005, Peters
542 *et al.*, 2007). Some individuals in our analysis showed more pronounced and unpredictable changes. In
543 these individuals, the dominant *var* gene being expressed changed within one cycle of cultivation. This
544 implies short-term culture can result in unpredictable *var* gene expression as observed previously using a
545 semi-quantitative RT-PCR approach (Bachmann *et al.*, 2011) and that one would need to confirm *in vivo*
546 expression matches *in vitro* expression. This can be achieved using the assembly approach described here.

547 We observed no generalised pattern of up- or downregulation of specific *var* groups following transition to
548 culture. This implies there is probably not a selection event occurring during culture but may represent a
549 loss of selection that is present *in vivo.* A global down regulation of certain *var* groups might only occur as a
550 selective process over many cycles in extended culture. Determining changes in *var* group expression levels
551 are difficult using degenerate qPCR primers bias and previous studies have found conflicting results in
552 terms of changes of expression of *var* groups through cultivation. Zhang *et al.*, 2011 found a rapid
553 transcriptional decline of group A and group B *var* genes, however Peters *et al.*, 2007 found group A *var*
554 genes to have a high rate of downregulation, when compared to group B *var* genes. These studies differed
555 in the stage distribution of the parasites and were limited in measuring enough variants through their use
556 of primers. Our new approach allowed for the identification of more sequences, with 26.6% of assembled
557 DBLα domains not found via the DBLα-tag approach. This better coverage of the expressed *var* diversity
558 was not possible in these previous studies and may explain discrepancies observed.

559 Generally, there was a high consensus between all levels of *var* gene analysis and changes observed during
560 short-term *in vitro* cultivation. However, the impact of short-term culture was the most apparent at the *var*
561 transcript level and became less clear at higher levels. This highlights the need for accurate
562 characterisation of full length *var* transcripts and analysis of the *var* transcriptome at different levels, both
563 of which can be achieved with the new approach developed here.

564 We saw striking changes in the core gene transcriptomes between *ex vivo* and generation 1 parasites with
565 19% of the core genome being differentially expressed. A previous study showed that expression of 18% of
566 core genes were significantly altered after ~50 cycles through culture (Mackinnon *et al.*, 2009), but our
567 data suggest that much of this change occurs early in the transition to culture. We observed genes with
568 functions unrelated to ring-stage parasites were among those most significantly expressed in the
569 generation 1 vs *ex vivo* analysis, suggesting the culture conditions may temporarily dysregulate stage-
570 specific expression patterns or result in the parasites undergoing a rapid adaptation response (Andreadaki
571 *et al.*, 2020, Beeson *et al.*, 2016). Several AP2 transcription factors (AP2-SP2, AP2-EXP2, AP2-LT, AP2-O and
572 AP2-HC) were upregulated in generation 1. AP2-HC has been shown to be expressed in asexual parasites
573 (Carrington *et al.*, 2021). AP2-O is thought to be specific for the ookinete stage and AP2-SP2 plays a key
574 role in sporozoite stage specific gene expression (Kaneko *et al.*, 2015, Yuda *et al.*, 2010). Our findings are
575 consistent with another study investigating the impact of long-term culture (Mackinnon *et al.*, 2009) which
576 also found genes like merozoite surface proteins differentially expressed, however they were
577 downregulated in long-term cultured parasites, whereas we found them upregulated in generation 1. This
578 suggests short-term cultured parasites might be transcriptionally different from long-term cultured
579 parasites, especially in their invasion capabilities, something previously unobserved. Several genes involved
580 in the stress response of parasites were upregulated in generation 1, for example DnaJ proteins, serine

581 proteases and ATP dependent CLP proteases (Oakley *et al.*, 2007). The similarity of the core transcriptomes
582 of the *in vitro* samples compared to the heterogeneity seen in the *ex vivo* samples could be explained by a
583 stress response upon entry to culture. Studies investigating whether the dysregulation of stage specific
584 expression and the expression of stress associated genes persist in long-term culture are required to
585 understand whether they are important for growth in culture. Critically, the marked differences presented
586 here suggest the impact of short-term culture can override differences observed in both the *in vivo* core
587 and *var* transcriptomes of different disease manifestations.

588 In summary, we present an enhanced approach for *var* transcript assembly which allows for *var* gene
589 expression to be studied in connection to *P. falciparum's* core transcriptome through RNA-sequencing. This
590 will be useful for expanding our understanding of *var* gene regulation and function in *in vivo* samples. As an
591 example of the capabilities of the new approach, the method was used to quantify differences in gene
592 expression upon short-term culture adaptation. This revealed that inferences from clinical isolates of *P.*
593 *falciparum* put into short-term culture must be made with a degree of caution. Whilst *var* gene expression
594 is often maintained, unpredictable switching does occur, necessitating that the similarity of *in vivo* and *in*
595 *vitro* expression should be confirmed. The more extreme changes in the core transcriptome could have
596 much bigger implications for understanding other aspects of parasite biology such as growth rates and
597 drug susceptibility and raise a need for additional caution. Further work is needed to examine *var* and core
598 transcriptome changes during longer term culture on a larger sample size. Understanding the ground truth
599 of the *var* expression repertoire of *Plasmodium* field isolates still presents a unique challenge and this work
600 expands the database of *var* sequences globally. The increase in long-read sequencing and the growing size
601 of *var* gene databases containing isolates from across the globe will help overcome this issue in future
602 studies.
603
604 **Materials and Methods**
605
606 **Ethics statement**
607 The study was conducted according to the principles of the Declaration of Helsinki, 6th edition, and the
608 International Conference on Harmonization-Good Clinical Practice (ICH-GCP) guidelines. All 32 patients
609 were treated as inpatients or outpatients in Hamburg, Germany (outpatient clinic of the University Medical
610 Center Hamburg-Eppendorf (UKE) at the Bernhard Nocht Institute for Tropical Medicine, UKE,
611 Bundeswehrkrankenhaus) (Wichers *et al.*, 2021). Blood samples for this analysis were collected after
612 patients had been informed about the aims and risks of the study and had signed an informed consent
613 form for voluntary blood collection (n=21). In the remaining cases, no intended blood samples were
614 collected but residuals from diagnostic blood samples were used (n=11). The study was approved by the
615 responsible ethics committee (Ethics Committee of the Hamburg Medical Association, reference numbers
616 PV3828 and PV4539).
617
618 **Blood sampling, processing and *in vitro* cultivation of *P. falciparum***
619 EDTA blood samples (1–30 mL) were collected from 32 adult falciparum malaria patients for *ex vivo*
620 transcriptome profiling as reported by Wichers et al., 2021 (Wichers *et al.*, 2021), hereafter termed 'the
621 original analysis'. Erythrocytes were isolated by Ficoll gradient centrifugation, followed by filtration
622 through Plasmodipur filters (EuroProxima) to remove residual granulocytes. At least 400 µl of the purified
623 erythrocytes were quickly lysed in 5 volumes of pre-warmed TRIzol (ThermoFisher Scientific) and stored at
624 -80°C until further processing ("*ex vivo* samples"). When available, the remainder was then transferred to
625 *in vitro* culture either without the addition of allogeneic red cells or with the addition of O+ human red
626 cells (blood bank, UKE) for dilution according to a protocol adopted from Trager and Jensen (Table S4).
627 Cultures were maintained at 37°C in an atmosphere of 1% O2, 5% CO2, and 94% N2 using RPMI complete
628 medium containing 10% heat-inactivated human serum (A+, Interstate Blood Bank, Inc., Memphis, USA).

629 Cultures were sampled for RNA purification at the ring stage by microscopic observation of the individual
630 growth of parasite isolates, and harvesting was performed at the appropriate time without prior
631 synchronization treatment ("*in vitro* samples"). 13 of these *ex vivo* samples underwent one cycle of *in vitro*
632 cultivation, ten of these generation 1 samples underwent a second cycle of *in vitro* cultivation. One of
633 these generation 2 samples underwent a third cycle of *in vitro* cultivation (Table 1). In addition, an aliquot
634 of *ex vivo* erythrocytes (approximately 50–100 µl) and aliquots of *in vitro* cell cultures collected as
635 indicated in Supplementary file 4 were processed for gDNA purification and MSP1 genotyping as described
636 elsewhere (Wichers *et al.*, 2021, Robert *et al.*, 1996).
637
638 **RNA purification, RNA-sequencing library preparation, and sequencing**
639 RNA purification was performed as described in Wichers *et al.*, 2021, using TRIzol in combination with the
640 RNeasy MinElute Kit (Qiagen) and DNase digestion (DNase I, Qiagen). Human globin mRNA was depleted
641 from all samples except from samples #1 and #2 using the GLOBINclear kit (ThermoFisher Scientific). The
642 median RIN value over all *ex vivo* samples was 6.75 (IQR: 5.93–7.40), although this measurement has only
643 limited significance for samples containing RNA of two species. Accordingly, the RIN value increased upon
644 cultivation for all *in vitro* samples (Supplementary file 5). Customized library construction in accordance to
645 Tonkin-Hill *et al.,* 2018, including amplification with KAPA polymerase and HiSeq 2500 125 bp paired-end
646 sequencing was performed by BGI Genomics Co. (Hong Kong).
647
648 **Methods for assembling *var* genes**
649 Previously Oases, Velvet, SoapDeNovo-Trans or MaSuRCA have been used for *var* transcript assembly
650 (Wichers *et al.*, 2021, Andrade *et al.*, 2020, Otto *et al.*, 2019, Tonkin-Hill *et al.*, 2018). Previous methods
651 either did not incorporate read error correction or focussed on gene assembly, as opposed to transcript
652 assembly (Schulz *et al.*, 2012, Zerbino & Birney, 2008, Xie *et al.*, 2014, Zimin *et al.*, 2013). Read error
653 correction is important for *var* transcript assembly due to the highly repetitive nature of the *P. falciparum*
654 genome. Recent methods have also focused on whole transcript assembly, as opposed to initial separate
655 domain assembly followed by transcript assembly (Wichers *et al.*, 2021, Andrade *et al.*, 2020, Otto *et al.*,
656 2019, Tonkin-Hill *et al.*, 2018). The original analysis used SoapDeNovo-Trans to assemble the *var*
657 transcripts, however it is currently not possible to run all steps in the original approach, due to certain
658 tools being improved and updated. Therefore, SoapDeNovo-Trans (k=71) was used and termed the original
659 approach.
660
661 Here, two novel methods for whole *var* transcript and *var* domain assembly were developed and their
662 performance was evaluated in comparison to the original approach (Figure 2b). In both methods the reads
663 were first mapped to the human g38 genome and any mapped reads were removed. Next, the unmapped
664 reads were mapped to a modified *P. falciparum* 3D7 genome with *var* genes removed, to identify multi-
665 mapping reads commonly present in *Plasmodium* RNA-sequencing datasets. Any mapped reads were
666 removed. In parallel, the unmapped RNA reads from the human mapping stage were mapped against a
667 reference of field isolate *var* exon 1 sequences and the mapped reads identified (Otto *et al.*, 2019). These
668 reads were combined with the unmapped reads from the 3D7 genome mapping stage and duplicate reads
669 removed. All mapping was performed using sub-read align as in the original analysis (Wichers *et al.*, 2021).
670 The reads identified at the end of this process are referred to as "non-core reads".
671
672 **Whole *var* transcript and *var* domain assembly methods**
673 For whole *var* transcript assembly the non-core reads, for each sample separately, were assembled using
674 rnaSPAdes (k-mer =71, read_error_correction on) (Bushmanova *et al.*, 2019). Contigs were joined into
675 larger scaffolds using SSPACE (parameters -n 31 -x 0 -k 10) (Boetzer *et al.*, 2011). Transcripts < 500nt were
676 excluded, as in the original approach. The included transcripts were annotated using hidden Markov
677 models (HMM) (Finn *et al.*, 2011) built on the *Rask et al.*, 2010 dataset and used in Tonkin-Hill *et al.*, 2018.

When annotating the whole transcript, the most significant alignment was taken as the best annotation for each region of the assembled transcript (e-value cut off 1e-5). Multiple annotations were allowed on the transcript if they were not overlapping, determined using cath-resolve-hits (Lewis *et al.*, 2019). Scripts are available in the GitHub repository (https://github.com/ClareAndradiBrown/varAssembly)

In the *var* domain assembly approach, separate domains were assembled first and then joined up to form transcripts. First, the non-core reads were mapped (nucleotide basic local alignment tool (blastn) short read option) to the domain sequences as defined in Rask *et al.*, 2010. This was found to produce similar results when compared to using tblastx. An e-value threshold of 1e-30 was used for the more conserved DBLα domains and an e-value of 1e-10 for the other domains. Next, the reads mapping to the different domains were assembled separately. rnaSPAdes (read_error_correction on, k-mer = 15), Oases (kmer = 15) and SoapDeNovo2 (kmer = 15) were all used to assemble the reads separately (Bushmanova *et al.*, 2019, Xie *et al.*, 2014, Schulz *et al.*, 2012). The output of the different assemblers was combined into a per sample reference of domain sequences. Redundancy was removed in the reference using cd-hit (-n 8-c 0.99) (at sequence identity = 99%) (Fu *et al.*, 2012). Cap3 was used to merge and extend the domain assemblies (Huang & Madan, 1999). SSPACE was used to join the domains together (parameters -n 31 -x 0 -k 10) (Boetzer *et al.*, 2011). Transcript annotation was performed as in the whole transcript approach, with transcripts < 500 nt removed. Significantly annotated (1e-5) transcripts were identified and selected. The most significant annotation was selected as the best annotation for each region, with multiple annotations allowed on a single transcript if the regions were not overlapping. For both methods, a *var* transcript was selected if it contained at least one significantly annotated domain (in exon 1). *Var* transcripts that encoded only the more conserved exon 2 (acidic terminal segment (ATS) domain) were discarded.

Validation on RNA-sequencing dataset from *P. falciparum* reference strain 3D7

Both new approaches and the original approach (SoapDeNovo-Trans, k =71) (Wichers *et al.*, 2021, Tonkin-Hill *et al.*, 2018) were run on a public RNA-sequencing dataset of the intra-erythrocytic life cycle stages of cultured *P. falciparum* 3D7 strain, sampled at 8-hr intervals up until 40 hrs post infection and then at 4 hr intervals up until 48 hrs post infection (ENA: PRJEB31535) (Wichers *et al.*, 2019). This provided a validation of all three approaches due to the true sequence of the *var* genes being known in *P. falciparum* 3D7 strain. Therefore, we compared the assembled sequences from all three approaches to the true sequence. The first best hit (significance threshold = 1e-10) was chosen for each contig. The alignment score was used to evaluate the performance of each method. The alignment score represents √accuracy* recovery. The accuracy is the proportion of bases that are correct in the assembled transcript and the recovery reflects what proportion of the true transcript was assembled. Misassemblies were counted as transcripts that had a percentage identity < 99% to their best hit (i.e. the *var* transcript is not 100% contained against the reference).

Comparison of approaches for *var* assembly on *ex vivo* samples

The *var* transcripts assembled from the 32 *ex vivo* samples using the original approach were compared to those produced from the whole transcript and domain assembly approaches. The whole transcript approach was chosen for subsequent analysis and all assembled *var* transcripts from this approach were combined into a reference, as in the original method (Wichers *et al.*, 2021).

Removal of *var* transcripts with sequence id >= 99% prior to mapping was not performed in the original analysis. To overcome this, *var* transcripts were removed if they had a sequence id >= 99% against the full complement in the whole transcript approach, using cd-hit-est (Fu *et al.*, 2012). Removing redundancy in the reference of assembled *var* transcripts across all samples led to the removal of 1,316 assembled contigs generated from the whole transcript approach.

This reference then represented all assembled *var* transcripts across all samples in the given analysis. The non-core reads were mapped against this reference and quantification was performed using Salmon (Patro

726 *et al.*, 2017). DESeq2 was used to perform differential expression analysis between severe versus non-
727 severe groups and naïve versus pre-exposed groups (Love *et al.*, 2014).
728 The assembled *var* transcripts produced by the whole transcript assembly approach had their expression
729 quantified at the transcript and domain level, as in the original method, and the results were compared to
730 those obtained by the original method. To quantify domain expression, featureCounts was used, as in the
731 original method with the counts for each domain aggregated (Liao *et al.*, 2014). Correlation analysis
732 between the domain's counts from the whole transcript approach and the original method was performed
733 for each *ex vivo* sample. Differential expression analysis was also performed using DESeq2, as in the
734 original analysis and the results compared (Love *et al.*, 2014, Wichers *et al.*, 2021).
735
736 **Estimation of parasite lifecycle stage distribution in *ex vivo* and short-term *in vitro* samples**
737 To determine the parasite life cycle stage proportions for each sample the mixture model approach of the
738 original analysis (Tonkin-Hill *et al.*, 2018, Wichers *et al.*, 2021) and the SCDC approach were used (Dong *et*
739 *al.*, 2021, Howick *et al.*, 2019). Recently, it has been determined that species-agnostic reference datasets
740 can be used for efficient and accurate gene expression deconvolution of bulk RNA-sequencing data from
741 any *Plasmodium* species and for correct gene expression analyses for biases caused by differences in stage
742 composition among samples (Tebben *et al.*, 2022). Therefore, the *Plasmodium berghei* single cell atlas was
743 used as reference with restriction to 1:1 orthologs between *P. berghei* and *P. falciparum*. This reference
744 was chosen as it contained reference transcriptomes for the gametocyte stage. To ensure consistency with
745 the original analysis, proportions from the mixture model approach were used for all subsequent analyses
746 (Wichers *et al.*, 2021). For comparison, the proportion of different stages of the parasite life cycle in the *ex*
747 *vivo* and *in vitro* samples was determined by two independent readers in Giemsa-stained thin blood
748 smears. The same classification as the mixture model approach was used (8, 19, 30, and 42 hours post
749 infection corresponding to ring, early trophozoite, late trophozoite and schizont stages respectively).
750 Significant differences in ring stage proportions were tested using pairwise Wilcoxon tests. For the other
751 stages, a modified Wilcoxon rank test for zero-inflated data was used (Wang *et al.*, 2021).
752
753 **Differential expression of *var* transcripts and domains from *ex vivo* to *in vitro* samples**
754 The whole transcript approach was applied to the paired *ex vivo* and *in vitro* samples. Significant
755 differences in the number of assembled *var* transcripts and the length of the transcripts across the
756 generations was tested using the paired Wilcoxon test.
757 Redundancy was removed from the assembled *var* transcripts and transcripts and domains were
758 quantified using the approach described above. Three additional filtering steps were applied separately to
759 this reference of assembled *var* transcripts to ensure the *var* transcripts that went on to have their
760 expression quantified represented true *var* transcripts. The first method restricted *var* transcripts to those
761 greater than 1500nt containing at least 3 significantly annotated *var* domains, one of which had to be a
762 DBLα domain. The second restricted *var* transcripts to those greater than 1500nt and containing a DBLα
763 domain. The third approach restricted *var* transcripts to those greater than 1500nt with at least 3
764 significant *var* domain annotations. Domain expression was quantified using featureCounts, as described
765 above (Liao *et al.*, 2014).
766 DESeq2 was used to test for differential transcript and domain expression, with five expected read counts
767 in at least three patient isolates required, with life cycle stage and patient identity used as covariates. For
768 the *ex vivo* versus *in vitro* comparisons, only *ex vivo* samples that had paired samples in generation 1
769 underwent differential expression analysis, given the extreme nature of the polymorphism seen in the *var*
770 genes. Differential expression analysis was performed for all three filtering methods described above.
771 Differential expression analysis was also performed using samples that had a single MSP1 genotype, to
772 ensure differences observed were not a consequence of having multiple *Plasmodium* genotypes present
773 (Love *et al.*, 2014).

774 To check for the differential expression of conserved *var* gene variants *var1-3D7*, *var1-IT* and *var2csa*, all
775 assembled transcripts significantly annotated as such were identified. For each conserved gene, Salmon
776 normalised read counts (adjusted for life cycle stage) were summed and expression compared across the
777 generations using a pairwise Wilcoxon rank test.
778
779 **Per patient *var* transcript expression**
780 A limitation of *var* transcript differential expression analysis is that it assumes all *var* sequences have the
781 possibility of being expressed in all samples. However, since each parasite isolate has a different set of *var*
782 gene sequences, this assumption is not completely valid. To account for this, *var* transcript expression
783 analysis was performed on a per patient basis. For each patient, the paired *ex vivo* and *in vitro* samples
784 were analysed. The assembled *var* transcripts (at least 1500nt and containing 3 significantly annotated *var*
785 domains) across all the generations for a patient were combined into a reference, redundancy was
786 removed as described above, and expression was quantified using Salmon (Patro *et al.*, 2017). *Var*
787 transcript expression was ranked, and the rankings compared across the generations.
788
789 ***Var* expression homogeneity (VEH)**
790 VEH is defined as the extent to which a small number of *var* gene sequences dominate an isolate's
791 expression profile (Warimwe *et al.*, 2013). Previously, this has been evaluated by calculating a commonly
792 used α diversity index, the Simpson's index of diversity. Different α diversity indexes put different weights
793 on evenness and richness. To overcome the issue of choosing one metric, α diversity curves were
794 calculated (Wagner *et al.*, 2018). Equation 1 is the computational formula for diversity curves. *D* is
795 calculated for *q* in the range 0 to 3 with a step increase of 0.1 and *p* in this analysis represented the
796 proportion of *var* gene expression dedicated to *var* transcript *k*. *q* determined how much weight is given to
797 rare vs abundant *var* transcripts. The smaller the *q* value, the less weight was given to the more abundant
798 *var* transcript. VEH was investigated on a per patient basis. The Bray-Curtis β diversity index was also
799 calculated across all samples. Bray-Curtis measures the dissimilarity between samples and was chosen for
800 its ability to handle absences of certain transcripts (Jari Oksanen, 2018).
801
802
803
804 Equation 1 $$D_{(q)} = \left(\sum_{k=1}^{K} p_k^q\right)^{\frac{1}{1-q}}$$
805
806
807
808 ***Var* group expression analysis**
809 The type of the *var* gene is determined by multiple parameters: upstream sequence (ups), chromosomal
810 location, direction of transcription and domain composition. All regular *var* genes encode a DBLα domain
811 in the N-terminus of the PfEMP1 protein (Figure 1c). The type of this domain correlates with previously
812 defined *var* gene groups, with group A encoding DBLα1, groups B and C encoding DBLα0 and group B
813 encoding a DBLα2 (chimera between DBLα0 and DBLα1)(Figure 1c). The DBLα domain sequence for each
814 transcript was determined and for each patient a reference of all assembled DBLα domains combined. The
815 relevant sample's non-core reads were mapped to this using Salmon and DBLα expression quantified
816 (Patro *et al.*, 2017). DESeq2 normalisation was performed, with patient identity and life cycle stage
817 proportions included as covariates and differences in the amounts of *var* transcripts of group A compared
818 with groups B and C assessed (Love *et al.*, 2014). A similar approach was repeated for NTS domains. NTSA
819 domains are found encoded in group A *var* genes and NTSB domains are found encoded in group B and C
820 *var* genes (Figure 1c).
821
822 **Quantification of total *var* gene expression**

823 The RNA-sequencing reads were blastn (with the short-blastn option on and significance = 1e-10) against
824 the LARSFADIG nucleotide sequences (142 unique LARSFADIG sequences) to identify reads containing the
825 LARSFADIG motifs. This approach has been described previously (Andrade *et al.*, 2020). Once the reads
826 containing the LARSFADIG motifs had been identified, they were used to assembled the LARSFADIG motif.
827 Trinity (Henschel, 2012) and rnaSPAdes (Bushmanova *et al.*, 2019) were used separately to assemble the
828 LARSFADIG motif, and the results compared. The sequencing reads were mapped back against the
829 assemblies using bwa mem (Li, 2013), parameter -k 31 -a (as in Andrade *et al.*, 2020). Coverage over the
830 LARSFADIG motif was assessed by determining the coverage over the middle of the motif (S) using
831 Samtools depth (Danecek *et al.*, 2021). These values were divided by the number of reads mapped to the
832 *var* exon 1 database and the 3D7 genome (which had *var* genes removed) to represent the proportion of
833 total gene expression dedicated to *var* gene expression (similar to an RPKM). The results of both
834 approaches were compared. This method has been validated on 3D7, IT and HB3 *Plasmodium* strains.
835 Significant differences in total *var* gene expression were tested by constructing a linear model with the
836 proportion of gene expression dedicated to *var* gene expression as the explanatory variable, the
837 generation and life cycle stage as an independent variables and the patient identity included as a random
838 effect.
839
840 ***Var* expression profiling by DBLα-tag sequencing**
841 DBLα-tag sequence analysis was performed as in the original analysis (Wichers *et al.*, 2021), with Varia
842 used to predict domain composition (Mackenzie *et al.*, 2022). The proportion of transcripts encoding NTSA,
843 NTSB, DBLα1, DBLα2 and DBLα0 domains were determined for each sample. These expression levels were
844 used as an alternative approach to see whether there were changes in the *var* group expression levels
845 through culture.
846
847 The consistency of domain annotations was also investigated between the DBLα-tag approach and the
848 assembled transcripts. This was investigated on a per patient basis, with all the predicted annotations from
849 the DBLα-tag approach for a given patient combined. These were compared to the annotations from all
850 assembled transcripts for a given patient. DBLα annotations and DBLα-CIDR annotations were compared.
851
852 For comparison of both approaches (DBLα-tag sequencing and our new whole transcript approach), the
853 same analysis was performed as in the original analysis (Wichers *et al.*, 2021). All conserved variants (*var1,*
854 *var2csa* and *var3*) were removed as they were not properly amplified by the DBLα-tag approach. To
855 identify how many assembled transcripts, specifically the DBLα region, were found in the DBLα-tag
856 approach, we applied BLAST. As in the original analysis, a BLAST database was created from the DBLα-tag
857 cluster results and screened for the occurrence of those assembled DBLα regions with more than 97% seq
858 id using the 'megablast' option. This was restricted to the assembled DBLα regions that were expressed in
859 the top 75th percentile to allow for a fair comparison, as only DBLα-tag clusters with more than 10 reads
860 were considered. Similarly, to identify how many DBLα-tag sequences were found in the assembled
861 transcripts, a BLAST database was created from the assembled transcripts and screened for the occurrence
862 of the DBLα-tag sequences with more than 97% seq id using the 'megablast' option. This was performed
863 for each sample.
864
865 **Core gene differential expression analysis**
866 Subread align was used, as in the original analysis, to align the reads to the human genome and *P.*
867 *falciparum* 3D7 genome, *with var, rif, stevor, surf* and *rRNA* genes removed (Liao *et al.*, 2013). HTSeq count
868 was used to quantify gene counts (Anders *et al.*, 2015). DESeq2 was used to test for differentially
869 expressed genes with five read counts in at least three samples being required (Love *et al.*, 2014). Parasite
870 life cycle stages and patient identity were included as covariates. GO and KEGG analysis was performed

using ShinyGo and significant terms were defined by having a Bonferroni corrected p-value < 0.05 (Ge *et al.*, 2020).

Funding / Acknowledgements

CAB received support from the Wellcome Trust (4-Year PhD programme, grant number 220123/Z/20/Z). Infrastructure support for this research was provided by the NIHR Imperial Biomedical Research Centre and Imperial College Research Computing Service, DOI: 10.14469/hpc/2232.
JSWM, YDH and AB were funded by the German Research Foundation (DFG) grants BA 5213/3-1 (project #323759012) and BA 5213/6-1 (project #433302244).
TO is supported by the Wellcome Trust grant 104111/Z/14/ZR. The funders had no role in study design, data collection and analysis, decision to publish, or preparation of the manuscript.
JB acknowledges support from Wellcome (100993/Z/13/Z)

Author contribution

Conceptualization: CAB, TDO, AB, AJC
Methodology: CAB, MFD, TL, TDO
Software: CAB
Validation: CAB, AB
Formal analysis: CAB
Investigation: JSW, HvT, YDH, JAMS, HSH, EFH, AB
Resources: TL, AJC, AB
Data curation: CAB, AB
Writing – original draft: CAB, TDO, AJC, AB
Writing – review & editing: CAB, JSW, MFD, TL, TWG, JB, TDO, AJC, AB
Visualization: CAB
Supervision: TWG, JB, TDO, AJC, AB
Project Administration: CAB, AJC, AB
Funding acquisition: AJC, AB

All authors read and approved the manuscript.

Competing interests

No competing interests declared.

References

Almelli, T., Nuel, G., Bischoff, E., Aubouy, A., Elati, M., Wang, C.W., Dillies, M.A., Coppee, J.Y., Ayissi, G.N., Basco, L.K., Rogier, C., Ndam, N.T., Deloron, P., and Tahar, R. (2014) Differences in gene transcriptomic pattern of Plasmodium falciparum in children with cerebral malaria and asymptomatic carriers. *PLoS One* **9**: e114401.

Anders, S., Pyl, P.T., and Huber, W. (2015) HTSeq--a Python framework to work with high-throughput sequencing data. *Bioinformatics* **31**: 166-169.

Andrade, C.M., Fleckenstein, H., Thomson-Luque, R., Doumbo, S., Lima, N.F., Anderson, C., Hibbert, J., Hopp, C.S., Tran, T.M., Li, S., Niangaly, M., Cisse, H., Doumtabe, D., Skinner, J., Sturdevant, D., Ricklefs, S., Virtaneva, K., Asghar, M., Homann, M.V., Turner, L., Martins, J., Allman, E.L., N'Dri, M.E., Winkler, V., Llinas, M., Lavazec, C., Martens, C., Farnert, A., Kayentao, K., Ongoiba, A., Lavstsen, T., Osorio, N.S., Otto, T.D., Recker, M., Traore, B., Crompton, P.D., and Portugal, S. (2020) Increased circulation time of Plasmodium falciparum underlies persistent asymptomatic infection in the dry season. *Nat Med* **26**: 1929-1940.

919 Andreadaki, M., Pace, T., Grasso, F., Siden-Kiamos, I., Mochi, S., Picci, L., Bertuccini, L., Ponzi, M., and Curra,
920 C. (2020) Plasmodium berghei Gamete Egress Protein is required for fertility of both genders.
921 *Microbiologyopen* **9**: e1038.
922 Avril, M., Tripathi, A.K., Brazier, A.J., Andisi, C., Janes, J.H., Soma, V.L., Sullivan, D.J., Jr., Bull, P.C., Stins,
923 M.F., and Smith, J.D. (2012) A restricted subset of var genes mediates adherence of Plasmodium
924 falciparum-infected erythrocytes to brain endothelial cells. *Proc Natl Acad Sci U S A* **109**: E1782-
925 1790.
926 Bachmann, A., Predehl, S., May, J., Harder, S., Burchard, G.D., Gilberger, T.W., Tannich, E., and Bruchhaus,
927 I. (2011) Highly co-ordinated var gene expression and switching in clinical Plasmodium falciparum
928 isolates from non-immune malaria patients. *Cell Microbiol* **13**: 1397-1409.
929 Baruch, D.I., Pasloske, B.L., Singh, H.B., Bi, X., Ma, X.C., Feldman, M., Taraschi, T.F., and Howard, R.J. (1995)
930 Cloning the P. falciparum gene encoding PfEMP1, a malarial variant antigen and adherence
931 receptor on the surface of parasitized human erythrocytes. *Cell* **82**: 77-87.
932 Beeson, J.G., Drew, D.R., Boyle, M.J., Feng, G., Fowkes, F.J., and Richards, J.S. (2016) Merozoite surface
933 proteins in red blood cell invasion, immunity and vaccines against malaria. *FEMS Microbiol Rev* **40**:
934 343-372.
935 Bernabeu, M., Danziger, S.A., Avril, M., Vaz, M., Babar, P.H., Brazier, A.J., Herricks, T., Maki, J.N., Pereira, L.,
936 Mascarenhas, A., Gomes, E., Chery, L., Aitchison, J.D., Rathod, P.K., and Smith, J.D. (2016) Severe
937 adult malaria is associated with specific PfEMP1 adhesion types and high parasite biomass. *Proc*
938 *Natl Acad Sci U S A* **113**: E3270-3279.
939 Boetzer, M., Henkel, C.V., Jansen, H.J., Butler, D., and Pirovano, W. (2011) Scaffolding pre-assembled
940 contigs using SSPACE. *Bioinformatics* **27**: 578-579.
941 Bozdech, Z., Llinas, M., Pulliam, B.L., Wong, E.D., Zhu, J., and DeRisi, J.L. (2003) The transcriptome of the
942 intraerythrocytic developmental cycle of Plasmodium falciparum. *PLoS Biol* **1**: E5.
943 Brown, A.C., and Guler, J.L. (2020) From Circulation to Cultivation: Plasmodium In Vivo versus In Vitro.
944 *Trends Parasitol* **36**: 914-926.
945 Bruske, E.I., Dimonte, S., Enderes, C., Tschan, S., Flotenmeyer, M., Koch, I., Berger, J., Kremsner, P., and
946 Frank, M. (2016) In Vitro Variant Surface Antigen Expression in Plasmodium falciparum Parasites
947 from a Semi-Immune Individual Is Not Correlated with Var Gene Transcription. *PLoS One* **11**:
948 e0166135.
949 Bushmanova, E., Antipov, D., Lapidus, A., and Prjibelski, A.D. (2019) rnaSPAdes: a de novo transcriptome
950 assembler and its application to RNA-Seq data. *Gigascience* **8**.
951 Carrington, E., Cooijmans, R.H.M., Keller, D., Toenhake, C.G., Bartfai, R., and Voss, T.S. (2021) The ApiAP2
952 factor PfAP2-HC is an integral component of heterochromatin in the malaria parasite Plasmodium
953 falciparum. *iScience* **24**: 102444.
954 Claessens, A., Adams, Y., Ghumra, A., Lindergard, G., Buchan, C.C., Andisi, C., Bull, P.C., Mok, S., Gupta,
955 A.P., Wang, C.W., Turner, L., Arman, M., Raza, A., Bozdech, Z., and Rowe, J.A. (2012) A subset of
956 group A-like var genes encodes the malaria parasite ligands for binding to human brain endothelial
957 cells. *Proc Natl Acad Sci U S A* **109**: E1772-1781.
958 Claessens, A., Affara, M., Assefa, S.A., Kwiatkowski, D.P., and Conway, D.J. (2017) Culture adaptation of
959 malaria parasites selects for convergent loss-of-function mutants. *Sci Rep* **7**: 41303.
960 Danecek, P., Bonfield, J.K., Liddle, J., Marshall, J., Ohan, V., Pollard, M.O., Whitwham, A., Keane, T.,
961 McCarthy, S.A., Davies, R.M., and Li, H. (2021) Twelve years of SAMtools and BCFtools. *Gigascience*
962 **10**.
963 Dimonte, S., Bruske, E.I., Hass, J., Supan, C., Salazar, C.L., Held, J., Tschan, S., Esen, M., Flotenmeyer, M.,
964 Koch, I., Berger, J., Bachmann, A., Sim, B.K., Hoffman, S.L., Kremsner, P.G., Mordmuller, B., and
965 Frank, M. (2016) Sporozoite Route of Infection Influences In Vitro var Gene Transcription of
966 Plasmodium falciparum Parasites From Controlled Human Infections. *J Infect Dis* **214**: 884-894.

967 Dong, M., Thennavan, A., Urrutia, E., Li, Y., Perou, C.M., Zou, F., and Jiang, Y. (2021) SCDC: bulk gene
968 expression deconvolution by multiple single-cell RNA sequencing references. *Brief Bioinform* **22**:
969 416-427.
970 Finn, R.D., Clements, J., and Eddy, S.R. (2011) HMMER web server: interactive sequence similarity
971 searching. *Nucleic Acids Res* **39**: W29-37.
972 Fu, L., Niu, B., Zhu, Z., Wu, S., and Li, W. (2012) CD-HIT: accelerated for clustering the next-generation
973 sequencing data. *Bioinformatics* **28**: 3150-3152.
974 Ge, S.X., Jung, D., and Yao, R. (2020) ShinyGO: a graphical gene-set enrichment tool for animals and plants.
975 *Bioinformatics* **36**: 2628-2629.
976 Guillochon, E., Fraering, J., Joste, V., Kamaliddin, C., Vianou, B., Houze, L., Baudrin, L.G., Faucher, J.F.,
977 Aubouy, A., Houze, S., Cot, M., Argy, N., Taboureau, O., Bertin, G.I., and Neuro, C.M.g. (2022)
978 Transcriptome Analysis of Plasmodium falciparum Isolates From Benin Reveals Specific Gene
979 Expression Associated With Cerebral Malaria. *J Infect Dis* **225**: 2187-2196.
980 Henschel, R., Lieber, M., Wu, L., Nista, P. M., Haas, B. J., LeDuc, R. D., (2012) Trinity RNA-Seq assembler
981 performance optimization. In: XSEDE '12: Proceedings of the 1st Conference of the Extreme Science
982 and Engineering Discovery Environment: Bridging from the eXtreme to the campus and beyond.
983 ACM, pp. 1-8.
984 Hoo, R., Bruske, E., Dimonte, S., Zhu, L., Mordmuller, B., Sim, B.K.L., Kremsner, P.G., Hoffman, S.L.,
985 Bozdech, Z., Frank, M., and Preiser, P.R. (2019) Transcriptome profiling reveals functional variation
986 in Plasmodium falciparum parasites from controlled human malaria infection studies. *EBioMedicine*
987 **48**: 442-452.
988 Howick, V.M., Russell, A.J.C., Andrews, T., Heaton, H., Reid, A.J., Natarajan, K., Butungi, H., Metcalf, T.,
989 Verzier, L.H., Rayner, J.C., Berriman, M., Herren, J.K., Billker, O., Hemberg, M., Talman, A.M., and
990 Lawniczak, M.K.N. (2019) The Malaria Cell Atlas: Single parasite transcriptomes across the complete
991 Plasmodium life cycle. *Science* **365**.
992 Huang, X., and Madan, A. (1999) CAP3: A DNA sequence assembly program. *Genome Res* **9**: 868-877.
993 Jari Oksanen, F., Friendly, M., Kindt, R., Legendre, P., McGlinn, D., Minchin, P. R., O'Hara, R. B., Simpson, G.
994 L., Solymos, P. & Stevens, M. H. H. , (2018) Vegan: community ecology package. *R Package Version.*
995 2 (6).
996 Jensen, A.T., Magistrado, P., Sharp, S., Joergensen, L., Lavstsen, T., Chiucchiuini, A., Salanti, A., Vestergaard,
997 L.S., Lusingu, J.P., Hermsen, R., Sauerwein, R., Christensen, J., Nielsen, M.A., Hviid, L., Sutherland, C.,
998 Staalsoe, T., and Theander, T.G. (2004) Plasmodium falciparum associated with severe childhood
999 malaria preferentially expresses PfEMP1 encoded by group A var genes. *J Exp Med* **199**: 1179-1190.
000 Jespersen, J.S., Wang, C.W., Mkumbaye, S.I., Minja, D.T., Petersen, B., Turner, L., Petersen, J.E., Lusingu,
001 J.P., Theander, T.G., and Lavstsen, T. (2016) Plasmodium falciparum var genes expressed in children
002 with severe malaria encode CIDRalpha1 domains. *EMBO Mol Med* **8**: 839-850.
003 Joste, V., Guillochon, E., Fraering, J., Vianou, B., Watier, L., Jafari-Guemouri, S., Cot, M., Houze, S., Aubouy,
004 A., Faucher, J.F., Argy, N., and Bertin, G.I. (2020) PfEMP1 A-Type ICAM-1-Binding Domains Are Not
005 Associated with Cerebral Malaria in Beninese Children. *mBio* **11**.
006 Kaneko, I., Iwanaga, S., Kato, T., Kobayashi, I., and Yuda, M. (2015) Genome-Wide Identification of the
007 Target Genes of AP2-O, a Plasmodium AP2-Family Transcription Factor. *PLoS Pathog* **11**: e1004905.
008 Kessler, A., Dankwa, S., Bernabeu, M., Harawa, V., Danziger, S.A., Duffy, F., Kampondeni, S.D., Potchen,
009 M.J., Dambrauskas, N., Vigdorovich, V., Oliver, B.G., Hochman, S.E., Mowrey, W.B., MacCormick,
010 I.J.C., Mandala, W.L., Rogerson, S.J., Sather, D.N., Aitchison, J.D., Taylor, T.E., Seydel, K.B., Smith,
011 J.D., and Kim, K. (2017) Linking EPCR-Binding PfEMP1 to Brain Swelling in Pediatric Cerebral Malaria.
012 *Cell Host Microbe* **22**: 601-614 e605.
013 Kirchgatter, K., and Portillo Hdel, A. (2002) Association of severe noncerebral Plasmodium falciparum
014 malaria in Brazil with expressed PfEMP1 DBL1 alpha sequences lacking cysteine residues. *Mol Med*
015 **8**: 16-23.

016 Kraemer, S.M., and Smith, J.D. (2003) Evidence for the importance of genetic structuring to the structural
017 and functional specialization of the Plasmodium falciparum var gene family. *Mol Microbiol* **50**:
018 1527-1538.
019 Kyes, S.A., Kraemer, S.M., and Smith, J.D. (2007) Antigenic variation in Plasmodium falciparum: gene
020 organization and regulation of the var multigene family. *Eukaryot Cell* **6**: 1511-1520.
021 Lavstsen, T., Magistrado, P., Hermsen, C.C., Salanti, A., Jensen, A.T., Sauerwein, R., Hviid, L., Theander, T.G.,
022 and Staalsoe, T. (2005) Expression of Plasmodium falciparum erythrocyte membrane protein 1 in
023 experimentally infected humans. *Malar J* **4**: 21.
024 Lavstsen, T., Salanti, A., Jensen, A.T., Arnot, D.E., and Theander, T.G. (2003) Sub-grouping of Plasmodium
025 falciparum 3D7 var genes based on sequence analysis of coding and non-coding regions. *Malar J* **2**:
026 27.
027 Lavstsen, T., Turner, L., Saguti, F., Magistrado, P., Rask, T.S., Jespersen, J.S., Wang, C.W., Berger, S.S.,
028 Baraka, V., Marquard, A.M., Seguin-Orlando, A., Willerslev, E., Gilbert, M.T., Lusingu, J., and
029 Theander, T.G. (2012) Plasmodium falciparum erythrocyte membrane protein 1 domain cassettes 8
030 and 13 are associated with severe malaria in children. *Proc Natl Acad Sci U S A* **109**: E1791-1800.
031 Lee, H.J., Georgiadou, A., Walther, M., Nwakanma, D., Stewart, L.B., Levin, M., Otto, T.D., Conway, D.J.,
032 Coin, L.J., and Cunnington, A.J. (2018) Integrated pathogen load and dual transcriptome analysis of
033 systemic host-pathogen interactions in severe malaria. *Sci Transl Med* **10**.
034 Leech, J.H., Barnwell, J.W., Miller, L.H., and Howard, R.J. (1984) Identification of a strain-specific malarial
035 antigen exposed on the surface of Plasmodium falciparum-infected erythrocytes. *J Exp Med* **159**:
036 1567-1575.
037 Lewis, T.E., Sillitoe, I., and Lees, J.G. (2019) cath-resolve-hits: a new tool that resolves domain matches
038 suspiciously quickly. *Bioinformatics* **35**: 1766-1767.
039 Li, H. (2013) Aligning sequence reads, clone sequences and assembly contigs with BWA-MEM. *arXiv*
040 *Preprint*: 1303.3997.
041 Liao, Y., Smyth, G.K., and Shi, W. (2013) The Subread aligner: fast, accurate and scalable read mapping by
042 seed-and-vote. *Nucleic Acids Res* **41**: e108.
043 Liao, Y., Smyth, G.K., and Shi, W. (2014) featureCounts: an efficient general purpose program for assigning
044 sequence reads to genomic features. *Bioinformatics* **30**: 923-930.
045 Lischer, H.E.L., and Shimizu, K.K. (2017) Reference-guided de novo assembly approach improves genome
046 reconstruction for related species. *BMC Bioinformatics* **18**: 474.
047 Love, M.I., Huber, W., and Anders, S. (2014) Moderated estimation of fold change and dispersion for RNA-
048 seq data with DESeq2. *Genome Biol* **15**: 550.
049 Mackenzie, G., Jensen, R.W., Lavstsen, T., and Otto, T.D. (2022) Varia: a tool for prediction, analysis and
050 visualisation of variable genes. *BMC Bioinformatics* **23**: 52.
051 Mackinnon, M.J., Li, J., Mok, S., Kortok, M.M., Marsh, K., Preiser, P.R., and Bozdech, Z. (2009) Comparative
052 transcriptional and genomic analysis of Plasmodium falciparum field isolates. *PLoS Pathog* **5**:
053 e1000644.
054 MalariaGen, Ahouidi, A., Ali, M., Almagro-Garcia, J., Amambua-Ngwa, A., Amaratunga, C., Amato, R.,
055 Amenga-Etego, L., Andagalu, B., Anderson, T.J.C., Andrianaranjaka, V., Apinjoh, T., Ariani, C., Ashley,
056 E.A., Auburn, S., Awandare, G.A., Ba, H., Baraka, V., Barry, A.E., Bejon, P., Bertin, G.I., Boni, M.F.,
057 Borrmann, S., Bousema, T., Branch, O., Bull, P.C., Busby, G.B.J., Chookajorn, T., Chotivanich, K.,
058 Claessens, A., Conway, D., Craig, A., D'Alessandro, U., Dama, S., Day, N.P., Denis, B., Diakite, M.,
059 Djimde, A., Dolecek, C., Dondorp, A.M., Drakeley, C., Drury, E., Duffy, P., Echeverry, D.F., Egwang,
060 T.G., Erko, B., Fairhurst, R.M., Faiz, A., Fanello, C.A., Fukuda, M.M., Gamboa, D., Ghansah, A.,
061 Golassa, L., Goncalves, S., Hamilton, W.L., Harrison, G.L.A., Hart, L., Henrichs, C., Hien, T.T., Hill, C.A.,
062 Hodgson, A., Hubbart, C., Imwong, M., Ishengoma, D.S., Jackson, S.A., Jacob, C.G., Jeffery, B.,
063 Jeffreys, A.E., Johnson, K.J., Jyothi, D., Kamaliddin, C., Kamau, E., Kekre, M., Kluczynski, K.,
064 Kochakarn, T., Konate, A., Kwiatkowski, D.P., Kyaw, M.P., Lim, P., Lon, C., Loua, K.M., Maiga-

065 Ascofare, O., Malangone, C., Manske, M., Marfurt, J., Marsh, K., Mayxay, M., Miles, A., Miotto, O.,
066 Mobegi, V., Mokuolu, O.A., Montgomery, J., Mueller, I., Newton, P.N., Nguyen, T., Nguyen, T.N.,
067 Noedl, H., Nosten, F., Noviyanti, R., Nzila, A.*, et al.* (2021) An open dataset of Plasmodium
068 falciparum genome variation in 7,000 worldwide samples. *Wellcome Open Res* **6**: 42.
069 Mkumbaye, S.I., Wang, C.W., Lyimo, E., Jespersen, J.S., Manjurano, A., Mosha, J., Kavishe, R.A.,
070 Mwakalinga, S.B., Minja, D.T.R., Lusingu, J.P., Theander, T.G., and Lavstsen, T. (2017) The Severity of
071 Plasmodium falciparum Infection Is Associated with Transcript Levels of var Genes Encoding
072 Endothelial Protein C Receptor-Binding P. falciparum Erythrocyte Membrane Protein 1. *Infect*
073 *Immun* **85**.
074 Mok, B.W., Ribacke, U., Rasti, N., Kironde, F., Chen, Q., Nilsson, P., and Wahlgren, M. (2008) Default
075 Pathway of var2csa switching and translational repression in Plasmodium falciparum. *PLoS One* **3**:
076 e1982.
077 Oakley, M.S., Kumar, S., Anantharaman, V., Zheng, H., Mahajan, B., Haynes, J.D., Moch, J.K., Fairhurst, R.,
078 McCutchan, T.F., and Aravind, L. (2007) Molecular factors and biochemical pathways induced by
079 febrile temperature in intraerythrocytic Plasmodium falciparum parasites. *Infect Immun* **75**: 2012-
080 2025.
081 Otto, T.D., Assefa, S.A., Bohme, U., Sanders, M.J., Kwiatkowski, D., Pf3k, c., Berriman, M., and Newbold, C.
082 (2019) Evolutionary analysis of the most polymorphic gene family in falciparum malaria. *Wellcome*
083 *Open Res* **4**: 193.
084 Patro, R., Duggal, G., Love, M.I., Irizarry, R.A., and Kingsford, C. (2017) Salmon provides fast and bias-aware
085 quantification of transcript expression. *Nat Methods* **14**: 417-419.
086 Peters, J.M., Fowler, E.V., Krause, D.R., Cheng, Q., and Gatton, M.L. (2007) Differential changes in
087 Plasmodium falciparum var transcription during adaptation to culture. *J Infect Dis* **195**: 748-755.
088 Pickford, A.K., Michel-Todo, L., Dupuy, F., Mayor, A., Alonso, P.L., Lavazec, C., and Cortes, A. (2021)
089 Expression Patterns of Plasmodium falciparum Clonally Variant Genes at the Onset of a Blood
090 Infection in Malaria-Naive Humans. *mBio* **12**: e0163621.
091 Quintana, M.D.P., Ecklu-Mensah, G., Tcherniuk, S.O., Ditlev, S.B., Oleinikov, A.V., Hviid, L., and Lopez-Perez,
092 M. (2019) Comprehensive analysis of Fc-mediated IgM binding to the Plasmodium falciparum
093 erythrocyte membrane protein 1 family in three parasite clones. *Sci Rep* **9**: 6050.
094 Rask, T.S., Hansen, D.A., Theander, T.G., Gorm Pedersen, A., and Lavstsen, T. (2010) Plasmodium
095 falciparum erythrocyte membrane protein 1 diversity in seven genomes--divide and conquer. *PLoS*
096 *Comput Biol* **6**.
097 Robert, F., Ntoumi, F., Angel, G., Candito, D., Rogier, C., Fandeur, T., Sarthou, J.L., and Mercereau-Puijalon,
098 O. (1996) Extensive genetic diversity of Plasmodium falciparum isolates collected from patients
099 with severe malaria in Dakar, Senegal. *Trans R Soc Trop Med Hyg* **90**: 704-711.
100 Rorick, M.M., Rask, T.S., Baskerville, E.B., Day, K.P., and Pascual, M. (2013) Homology blocks of Plasmodium
101 falciparum var genes and clinically distinct forms of severe malaria in a local population. *BMC*
102 *Microbiol* **13**: 244.
103 Sahu, P.K., Duffy, F.J., Dankwa, S., Vishnyakova, M., Majhi, M., Pirpamer, L., Vigdorovich, V., Bage, J.,
104 Maharana, S., Mandala, W., Rogerson, S.J., Seydel, K.B., Taylor, T.E., Kim, K., Sather, D.N., Mohanty,
105 A., Mohanty, R.R., Mohanty, A., Pattnaik, R., Aitchison, J.D., Hoffmann, A., Mohanty, S., Smith, J.D.,
106 Bernabeu, M., and Wassmer, S.C. (2021) Determinants of brain swelling in pediatric and adult
107 cerebral malaria. *JCI Insight* **6**.
108 Salanti, A., Dahlback, M., Turner, L., Nielsen, M.A., Barfod, L., Magistrado, P., Jensen, A.T., Lavstsen, T.,
109 Ofori, M.F., Marsh, K., Hviid, L., and Theander, T.G. (2004) Evidence for the involvement of
110 VAR2CSA in pregnancy-associated malaria. *J Exp Med* **200**: 1197-1203.
111 Scherf, A., Hernandez-Rivas, R., Buffet, P., Bottius, E., Benatar, C., Pouvelle, B., Gysin, J., and Lanzer, M.
112 (1998) Antigenic variation in malaria: in situ switching, relaxed and mutually exclusive transcription

113 of var genes during intra-erythrocytic development in Plasmodium falciparum. *EMBO J* **17**: 5418-
114 5426.
115 Schulz, M.H., Zerbino, D.R., Vingron, M., and Birney, E. (2012) Oases: robust de novo RNA-seq assembly
116 across the dynamic range of expression levels. *Bioinformatics* **28**: 1086-1092.
117 Shabani, E., Hanisch, B., Opoka, R.O., Lavstsen, T., and John, C.C. (2017) Plasmodium falciparum EPCR-
118 binding PfEMP1 expression increases with malaria disease severity and is elevated in retinopathy
119 negative cerebral malaria. *BMC Med* **15**: 183.
120 Smith, J.D., Chitnis, C.E., Craig, A.G., Roberts, D.J., Hudson-Taylor, D.E., Peterson, D.S., Pinches, R.,
121 Newbold, C.I., and Miller, L.H. (1995) Switches in expression of Plasmodium falciparum var genes
122 correlate with changes in antigenic and cytoadherent phenotypes of infected erythrocytes. *Cell* **82**:
123 101-110.
124 Stevenson, L., Laursen, E., Cowan, G.J., Bandoh, B., Barfod, L., Cavanagh, D.R., Andersen, G.R., and Hviid, L.
125 (2015) alpha2-Macroglobulin Can Crosslink Multiple Plasmodium falciparum Erythrocyte
126 Membrane Protein 1 (PfEMP1) Molecules and May Facilitate Adhesion of Parasitized Erythrocytes.
127 *PLoS Pathog* **11**: e1005022.
128 Storm, J., Jespersen, J.S., Seydel, K.B., Szestak, T., Mbewe, M., Chisala, N.V., Phula, P., Wang, C.W., Taylor,
129 T.E., Moxon, C.A., Lavstsen, T., and Craig, A.G. (2019) Cerebral malaria is associated with differential
130 cytoadherence to brain endothelial cells. *EMBO Mol Med* **11**.
131 Su, X.Z., Heatwole, V.M., Wertheimer, S.P., Guinet, F., Herrfeldt, J.A., Peterson, D.S., Ravetch, J.A., and
132 Wellems, T.E. (1995) The large diverse gene family var encodes proteins involved in cytoadherence
133 and antigenic variation of Plasmodium falciparum-infected erythrocytes. *Cell* **82**: 89-100.
134 Tarr, S.J., Diaz-Ingelmo, O., Stewart, L.B., Hocking, S.E., Murray, L., Duffy, C.W., Otto, T.D., Chappell, L.,
135 Rayner, J.C., Awandare, G.A., and Conway, D.J. (2018) Schizont transcriptome variation among
136 clinical isolates and laboratory-adapted clones of the malaria parasite Plasmodium falciparum. *BMC*
137 *Genomics* **19**: 894.
138 Taylor, H.M., Grainger, M., and Holder, A.A. (2002) Variation in the expression of a Plasmodium falciparum
139 protein family implicated in erythrocyte invasion. *Infect Immun* **70**: 5779-5789.
140 Tebben, K., Dia, A., and Serre, D. (2022) Determination of the Stage Composition of Plasmodium Infections
141 from Bulk Gene Expression Data. *mSystems* **7**: e0025822.
142 Tonkin-Hill, G.Q., Trianty, L., Noviyanti, R., Nguyen, H.H.T., Sebayang, B.F., Lampah, D.A., Marfurt, J.,
143 Cobbold, S.A., Rambhatla, J.S., McConville, M.J., Rogerson, S.J., Brown, G.V., Day, K.P., Price, R.N.,
144 Anstey, N.M., Papenfuss, A.T., and Duffy, M.F. (2018) The Plasmodium falciparum transcriptome in
145 severe malaria reveals altered expression of genes involved in important processes including
146 surface antigen-encoding var genes. *PLoS Biol* **16**: e2004328.
147 Tuikue Ndam, N., Moussiliou, A., Lavstsen, T., Kamaliddin, C., Jensen, A.T.R., Mama, A., Tahar, R., Wang,
148 C.W., Jespersen, J.S., Alao, J.M., Gamain, B., Theander, T.G., and Deloron, P. (2017) Parasites
149 Causing Cerebral Falciparum Malaria Bind Multiple Endothelial Receptors and Express EPCR and
150 ICAM-1-Binding PfEMP1. *J Infect Dis* **215**: 1918-1925.
151 Turner, L., Lavstsen, T., Berger, S.S., Wang, C.W., Petersen, J.E., Avril, M., Brazier, A.J., Freeth, J., Jespersen,
152 J.S., Nielsen, M.A., Magistrado, P., Lusingu, J., Smith, J.D., Higgins, M.K., and Theander, T.G. (2013)
153 Severe malaria is associated with parasite binding to endothelial protein C receptor. *Nature* **498**:
154 502-505.
155 Ukaegbu, U.E., Kishore, S.P., Kwiatkowski, D.L., Pandarinath, C., Dahan-Pasternak, N., Dzikowski, R., and
156 Deitsch, K.W. (2014) Recruitment of PfSET2 by RNA polymerase II to variant antigen encoding loci
157 contributes to antigenic variation in P. falciparum. *PLoS Pathog* **10**: e1003854.
158 Ukaegbu, U.E., Zhang, X., Heinberg, A.R., Wele, M., Chen, Q., and Deitsch, K.W. (2015) A Unique Virulence
159 Gene Occupies a Principal Position in Immune Evasion by the Malaria Parasite Plasmodium
160 falciparum. *PLoS Genet* **11**: e1005234.

161 Vignali, M., Armour, C.D., Chen, J., Morrison, R., Castle, J.C., Biery, M.C., Bouzek, H., Moon, W., Babak, T.,
162 Fried, M., Raymond, C.K., and Duffy, P.E. (2011) NSR-seq transcriptional profiling enables
163 identification of a gene signature of Plasmodium falciparum parasites infecting children. *J Clin*
164 *Invest* **121**: 1119-1129.
165 Wagner, B.D., Grunwald, G.K., Zerbe, G.O., Mikulich-Gilbertson, S.K., Robertson, C.E., Zemanick, E.T., and
166 Harris, J.K. (2018) On the Use of Diversity Measures in Longitudinal Sequencing Studies of Microbial
167 Communities. *Front Microbiol* **9**: 1037.
168 Wahlgren, M., Goel, S., and Akhouri, R.R. (2017) Variant surface antigens of Plasmodium falciparum and
169 their roles in severe malaria. *Nat Rev Microbiol* **15**: 479-491.
170 Wang, W., Chen, E.Z., and Li, H. (2021) Truncated Rank-Based Tests for Two-Part Models with Excessive
171 Zeros and Applications to Microbiome Data. *arXiv Preprint:2110.05368*.
172 Warimwe, G.M., Recker, M., Kiragu, E.W., Buckee, C.O., Wambua, J., Musyoki, J.N., Marsh, K., and Bull, P.C.
173 (2013) Plasmodium falciparum var gene expression homogeneity as a marker of the host-parasite
174 relationship under different levels of naturally acquired immunity to malaria. *PLoS One* **8**: e70467.
175 WHO, (2022) World malaria report. Geneva: World Health Organization.
176 Wichers, J.S., Scholz, J.A.M., Strauss, J., Witt, S., Lill, A., Ehnold, L.I., Neupert, N., Liffner, B., Luhken, R.,
177 Petter, M., Lorenzen, S., Wilson, D.W., Low, C., Lavazec, C., Bruchhaus, I., Tannich, E., Gilberger,
178 T.W., and Bachmann, A. (2019) Dissecting the Gene Expression, Localization, Membrane Topology,
179 and Function of the Plasmodium falciparum STEVOR Protein Family. *mBio* **10**.
180 Wichers, J.S., Tonkin-Hill, G., Thye, T., Krumkamp, R., Kreuels, B., Strauss, J., von Thien, H., Scholz, J.A.,
181 Smedegaard Hansson, H., Weisel Jensen, R., Turner, L., Lorenz, F.R., Schollhorn, A., Bruchhaus, I.,
182 Tannich, E., Fendel, R., Otto, T.D., Lavstsen, T., Gilberger, T.W., Duffy, M.F., and Bachmann, A.
183 (2021) Common virulence gene expression in adult first-time infected malaria patients and severe
184 cases. *Elife* **10**.
185 Xie, Y., Wu, G., Tang, J., Luo, R., Patterson, J., Liu, S., Huang, W., He, G., Gu, S., Li, S., Zhou, X., Lam, T.W., Li,
186 Y., Xu, X., Wong, G.K., and Wang, J. (2014) SOAPdenovo-Trans: de novo transcriptome assembly
187 with short RNA-Seq reads. *Bioinformatics* **30**: 1660-1666.
188 Yamagishi, J., Natori, A., Tolba, M.E., Mongan, A.E., Sugimoto, C., Katayama, T., Kawashima, S., Makalowski,
189 W., Maeda, R., Eshita, Y., Tuda, J., and Suzuki, Y. (2014) Interactive transcriptome analysis of
190 malaria patients and infecting Plasmodium falciparum. *Genome Res* **24**: 1433-1444.
191 Yang, X., Charlebois, P., Gnerre, S., Coole, M.G., Lennon, N.J., Levin, J.Z., Qu, J., Ryan, E.M., Zody, M.C., and
192 Henn, M.R. (2012) De novo assembly of highly diverse viral populations. *BMC Genomics* **13**: 475.
193 Yuda, M., Iwanaga, S., Shigenobu, S., Kato, T., and Kaneko, I. (2010) Transcription factor AP2-Sp and its
194 target genes in malarial sporozoites. *Mol Microbiol* **75**: 854-863.
195 Zerbino, D.R., and Birney, E. (2008) Velvet: algorithms for de novo short read assembly using de Bruijn
196 graphs. *Genome Res* **18**: 821-829.
197 Zhang, Q., Zhang, Y., Huang, Y., Xue, X., Yan, H., Sun, X., Wang, J., McCutchan, T.F., and Pan, W. (2011)
198 From in vivo to in vitro: dynamic analysis of Plasmodium falciparum var gene expression patterns of
199 patient isolates during adaptation to culture. *PLoS One* **6**: e20591.
200 Zhang, X., Florini, F., Visone, J.E., Lionardi, I., Gross, M.R., Patel, V., and Deitsch, K.W. (2022) A coordinated
201 transcriptional switching network mediates antigenic variation of human malaria parasites. *Elife* **11**.
202 Zimin, A.V., Marcais, G., Puiu, D., Roberts, M., Salzberg, S.L., and Yorke, J.A. (2013) The MaSuRCA genome
203 assembler. *Bioinformatics* **29**: 2669-2677.
204